Geofísica Internacional (1996), Vol. 35, Num. 1., pp. 3-25

Stratigraphy and geochronology of Miocene and Pliocene volcanic rocks in the Sierra San Fermín and southern Sierra San Felipe, Baja California, Mexico

Claudia J. Lewis
Department of Earth and Planetary Sciences, Harvard University, Cambridge, Massachusetts, USA.
Present Address: Departament de Geologia Dinàmica, Geofísica i Paleontologia, Universitat de Barcelona, Barcelona, Spain.

Received: October 10, 1994; accepted: August 14, 1995.

RESUMEN

La geología y geocronología ($^{40}Ar/^{39}Ar$) de la Sierra de San Fermín y parte meridional de la Sierra de San Felipe (Baja California) señalan volcanismo miocénico y pliocénico desde 21 Ma hasta por lo menos 3 Ma, dentro de un arco volcánico que se extendió a lo largo de la península debido a la subducción. El estudio abarca dos áreas eruptivas posteriores a la subducción (11 Ma y ~6 Ma), que fueron desgarradas por fallamiento normal y lateral izquierdo dentro de la Provincia del Golfo de California. Hacia 11 Ma, se depositó un derrame piroclástico regional de 40 m de espesor con andesitas locales y unidades epiclásticas. Hacia 6 Ma las erupciones cubrieron la región hasta espesores de 220 m de piroclásticos, cenizas, epiclásticos y derrames riolíticos locales. Las tobas aumentan en espesor hacia el sur y atraviesan una importante estructura de rumbo ENE que podría ser parte de una caldera en la Sierra de San Fermín, amontonándose contra esta barrera estructural; hacia el norte, escasean las tobas más jóvenes. Las discordancias angulares entre 11 Ma y 6 Ma indican la formación de grandes cuencas extensionales. Hubo un hiatus deposicional entre 11 Ma y ~6 Ma en gran parte del área de estudio; no obstante, hay afloramientos locales de 8 Ma. Probablemente se trate de un efecto de la topografía controlada por la caldera o por fallas normales y no de un período de baja actividad volcánica. De 6 Ma a 3 Ma se depositaron otros 600 m de riolitas y andesitas piroxénicas en las cuencas controladas por fallas.

PALABRAS CLAVE: Estratigrafía, geocronología, Provincia del Golfo de California, México.

ABSTRACT

Geological mapping and $^{40}Ar/^{39}Ar$ geochronology in the Sierra San Fermín and southern Sierra San Felipe (between latitudes 30°30' and 30°44' N and longitudes 114°42' and 114°51' W), northeastern Baja California, reveal a history of Miocene to Pliocene volcanism from 21 Ma to at least 3 Ma. The area is located within part of the early to middle Miocene, subduction–related volcanic arc which reached the length of the Baja California peninsula. The study area also straddles two major, post–subduction vent areas 11 and ~ 6 Ma in age which have been dismembered by normal and sinistral strike–slip faulting within the Gulf of California Extensional Province. Prior to 11 Ma, basement–derived arkosic sandstone, basalt and pyroclastic flows, and volcaniclastic sedimentary rocks locally covered Cretaceous and older batholithic and pre–batholithic rocks. Around 11 Ma, a 40–m thick regional pyroclastic flow, local hornblende andesite flows, and epiclastic volcanic units were deposited. At about 6 Ma, eruptions covered the region with an additional 220 m of pyroclastic flows, ash fall deposits, epiclastic volcanic units, and local rhyolite flows. Tuffs in this package thicken southwards across a major east-northeast–striking structure in the central Sierra San Fermín, which may be part of a caldera wall. The youngest of the tuffs in the 6 Ma sequence appear to have ponded against this structural barrier, causing the youngest units to be very thin or absent north of this boundary. Angular discordance between 11 and 6 Ma units indicates that major extensional basins formed in this time interval. A hiatus in deposition throughout much of the study area occurred between 11 Ma and ~6 Ma ago, although 8 Ma deposits crop out locally. This hiatus may not represent a lull in regional volcanic activity but merely the presence of local topography in the Sierra San Fermín with basins nearby, controlled by caldera collapse or normal faulting. Between 6 Ma and about 3 Ma, an additional 600 m of rhyolite and pyroxene andesite flows and breccias and pyroclastic flows were deposited in fault–controlled basins.

KEYWORDS: Stratigraphy, geochronology, Gulf Extensional Province, Mexico.

INTRODUCTION

The contemporaneity of volcanism and extension in northeastern Baja California make the northern Puertecitos Volcanic Province (Figure 1) an unparalleled natural laboratory for testing models of Neogene plate tectonic processes at the boundary between the Pacific and North America plates. Outstanding exposures of volcanic units provide a basis for unraveling the structural evolution of the northern Gulf of California Extensional Province. The area of study (Figure 1), between latitudes 30°30' and 30°44' N and longitudes 114°42' and 114°51' W (an area approximately 30 x 15 km) includes parts of two coastal ranges, the Sierra San Fermín and southern Sierra San Felipe, and the intervening valley (Llanos de San Fermín; Figure 2). Detailed geologic mapping of these areas was undertaken at a scale of 1:20,000. The objective of this report is to describe Tertiary units in the Sierra San Fermín and southern Sierra San Felipe and to present geochronological data from several of these units. Parts of the sequence of volcanic units correlate with previously studied late Miocene/Pliocene sequences in adjacent southern Valle Chico (Stock and Hodges, 1989) and Arroyo La Cantera/Valle Curbina west of Puertecitos (Stock *et al.*, 1991;

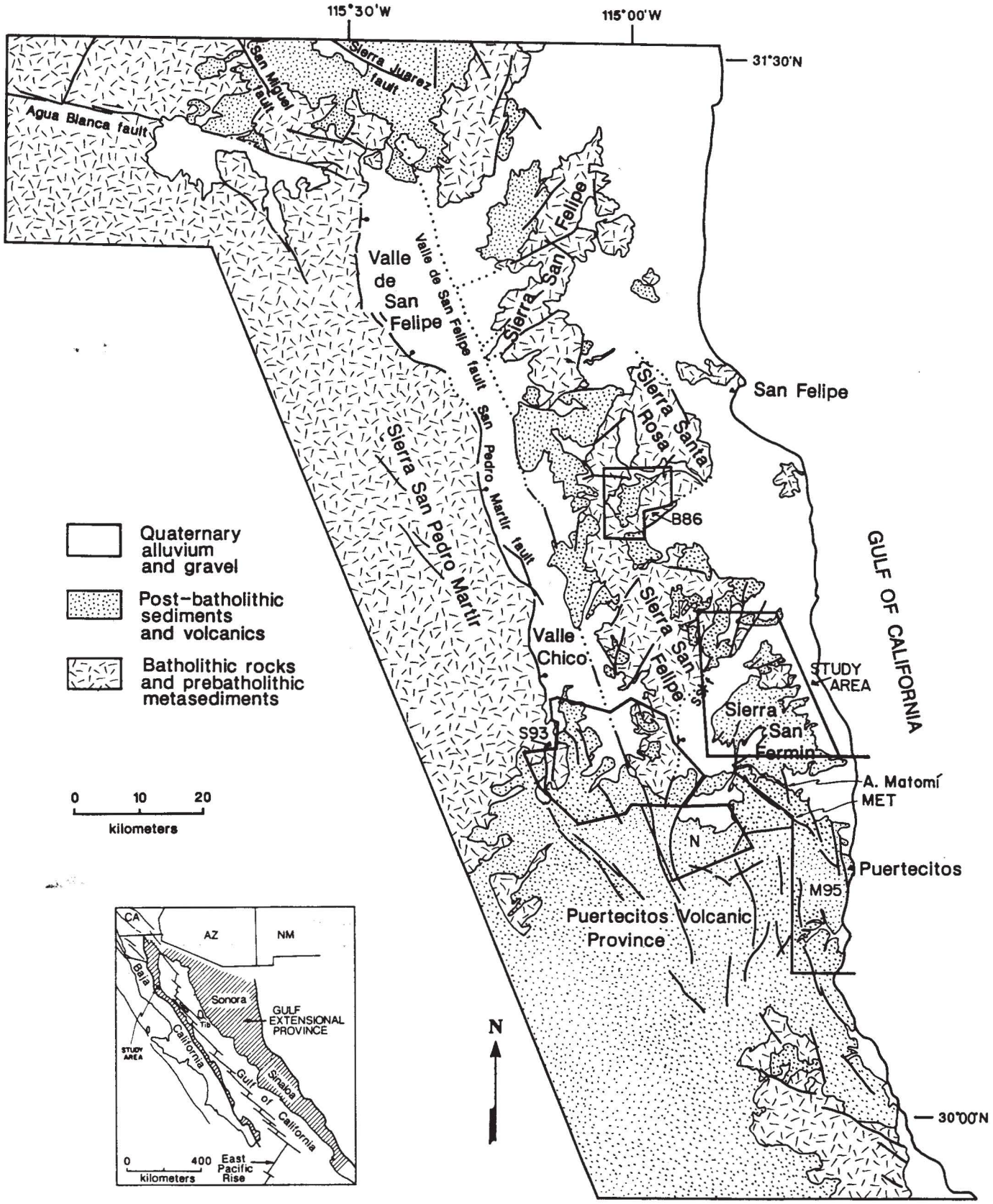

Fig. 1. Regional geologic map of part of northeastern Baja California, modified from Gastil *et al.* (1975), with present study area and areas of other major stratigraphic studies outlined—B86, Bryant (1986); M95, Martín-Barajas *et al.*, (1995); N, Elizabeth Nagy (PhD thesis in progress); S93, Stock (1993). Abbreviations: SSSf, Sierra San Felipe fault; MET, mesa El Tábano. Inset map shows present-day plate tectonic setting of northeastern Baja California. Abbreviation: Tib, Isla Tiburón.

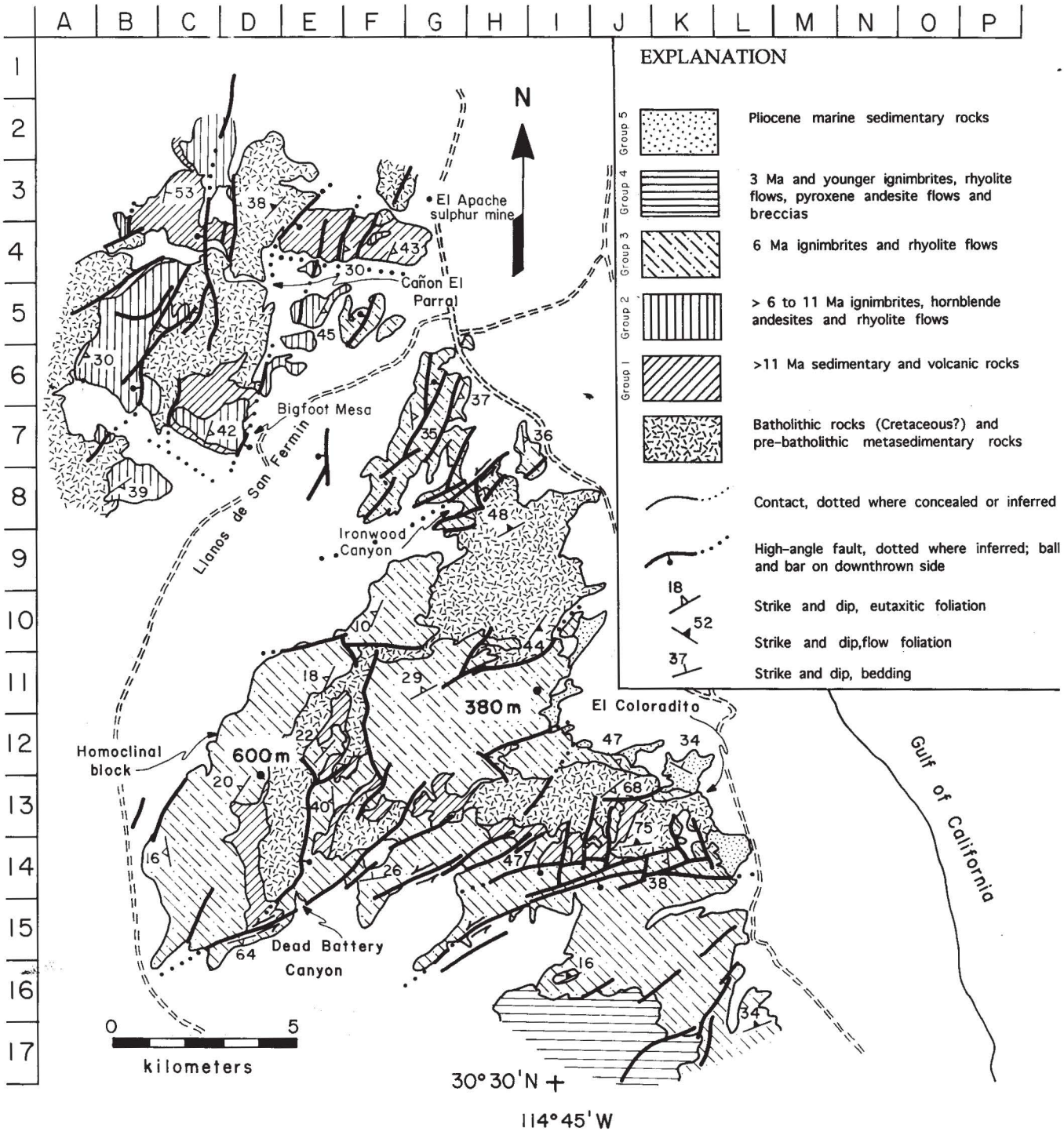

Fig. 2. Generalized geologic map of the study area (with strata grouped as in text), showing local geographic features. Orthogonal grid for reference to localities mentioned in text. Circles with labeled elevations mark post–11 Ma/pre–6 Ma basaltic andesite volcanoes.

Martín Barajas and Stock, 1993; Martín–Barajas *et al.*, 1995). The stratigraphy discussed in this paper documents the development of late Miocene volcanic centers within a zone of distributed dextral shear and provides kinematic constraints on the Miocene to Recent structural evolution of this area. These data constrain the timing of extension and strike–slip faulting and accompanying tectonic rotations about vertical axes, to be evaluated in subsequent papers on kinematics and paleomagnetics.

GEOLOGIC SETTING

The Sierra San Fermín and Sierra San Felipe lie on the eastern side of the Baja California peninsula in the state of

Baja California, Mexico (Figure 1). They are the hanging wall and footwall (respectively) of a major, east–dipping normal fault system, the Sierra San Felipe fault (new name; Figure 1), within the Gulf Extensional Province. These roughly north–striking parallel ranges are separated by the 6–km wide Llanos de San Fermín, a late Miocene to Recent extensional basin.

The western boundary of the Gulf Extensional Province (GEP) at this latitude is the Main Gulf Escarpment, which separates the relatively unextended batholithic rocks of the Peninsular Ranges, on the west, from the lower–elevation basins and ranges of the GEP to the east. The E–dipping San Pedro Mártir fault (Figure 1), the principal fault of the escarpment at this latitude, strikes approximately north-northwest for 80 km and has up to 5 km of normal separation (Gastil *et al.*, 1975; Dokka and Merriam, 1982).

The Escarpment becomes a more subduced topographic feature near the northern end of the Puertecitos Volcanic Province (PVP), where the overall strike of the fault system bounding this edge of the GEP changes from northerly to northwesterly (Figure 1). Displacement is transferred from the San Pedro Mártir fault onto multiple fault zones in the footwall, and small–displacement normal faults and subordinate transverse dextral faults in the hanging wall (Stock and Hodges, 1990). These structural and topographic changes mark a west–northwest–trending accommodation zone (Dokka and Merriam, 1982; Stock and Hodges, 1990), which may allow a reversal of upper plate transport direction within the GEP (Axen, 1995). This area is a locus of pre– and synextensional volcanism (e.g., Gastil *et al.*, 1979; Stock, 1989), which appears to be structurally controlled and related to development of the accommodation zone.

PREVIOUS WORK

The regional geology was summarized by previous investigators from aerial photographs (Gastil *et al.*, 1975; Dokka and Merriam, 1982), photographs taken from space (Hamilton, 1971), reconnaissance mapping, and unpublished master's theses by students at San Diego State University (Gastil *et al.*, 1975). Ages of some Tertiary units in northeastern Baja California were determined by K–Ar geochronology and paleontological studies (Sommer and Garcia, 1970; Andersen, 1973; Gastil *et al.*, 1975; Gastil *et al.*, 1979; Boehm, 1984; Bryant, 1986).

An informal stratigraphy has been worked out for areas directly west (southern Valle Chico) and south (eastern Puertecitos Volcanic Province) of the study area (Figure 1; Stock, 1989; Stock *et al.*, 1991; Martín Barajas and Stock, 1993; Martín Barajas *et al.*, 1993; Martín–Barajas *et al.*, 1995). Ages of Tertiary units were determined by K–Ar and $^{40}Ar/^{39}Ar$ geochronology for sections in these areas. This study follows and adds to the informal stratigraphy of Stock (1989) and Martín–Barajas *et al.* (1995).

TERTIARY STRATIGRAPHY

The post–batholithic strata of the Sierra San Fermín and the southern Sierra San Felipe are divided here into 5 informal units based on subtle but important unconformities associated with Neogene extensional and strike–slip faulting (Figures 2, 3). These are, from oldest to youngest: (1) sandstones, basalt flows, and epiclastic volcanic conglomerate; (2) 11 Ma welded ash flow tuff and andesites overlying the 11 Ma tuff; (3) pyroclastic flows, airfall and reworked deposits, and local rhyolite flows, with a 6.5 Ma tuff near the bottom of the section and a 6.4 Ma pumice flow near the top; (4) coalesced rhyolite domes and coulees, 3 Ma pyroclastic flows, and pyroxene andesite flows and breccias younger than 3 Ma; and (5) terrestrial and marine sedimentary rocks. The marine part of Group 5 will be described in a subsequent paper.

Compositional names have been assigned to the volcanic rocks based on phenocryst assemblages and textures following guidelines of Best (1982), and geochemical analyses of correlative units from adjacent areas (Martín–Barajas *et al.*, 1995; Stock, unpublished data). Black, olivine–bearing flows are labeled "basalt." Black to dark gray non–vesicular flows lacking olivine in thin–section, bearing plagioclase and hornblende, pyroxene, or biotite, and weathering in a platy or shaly fashion are labeled "basaltic andesite." Light gray and green– or pink–weathering flows bearing phenocrysts of plagioclase and quartz and mafic phenocrysts of any composition are labeled "dacite." Sparsely porphyritic, purple, red, brown, or gray aphanitic flows that are flow layered, associated with obsidian, block and glass flows, and lahars, and contain phenocrystic plagioclase, alkali feldspar, pyroxene, and vapor phase minerals trydimite and cristobalite are termed "rhyolite." Ignimbrites bearing phenocrysts of anorthoclase, quartz, and mafic phases are termed "rhyolite." Ignimbrites lacking anorthoclase but bearing plagioclase ± quartz and mafic phases are labeled "dacite" unless geochemical analyses justify calling them rhyolite. Pyroclastic deposits are classified by size following Fisher (1966).

Geochronological results are summarized in Table 1, illustrated in Figure 4, and discussed within unit descriptions below (see Appendix A for a description of the geochronological techniques). Thin section descriptions of each dated sample are provided in Appendix B, and measured sections of important units in Appendix C.

MIOCENE ROCKS

Group 1

Tertiary Basal Sandstones (Ts)

Extensive thin beds of poorly to moderately lithified arkosic sandstone and rare conglomerate (Ts) occur at the base of the Tertiary sequence (Figure 3; Lewis, 1994). Ts is typically recessive and covered by talus of overlying resistant volcanic units. Post–depositional tectonic tilting of Ts locally reaches 80° (E4, Figure 2).

In the west–central Sierra San Fermín (E12–13, Figure 2), residual arkose makes up the basal part of Ts, reaching thicknesses of several meters in paleotopographic lows.

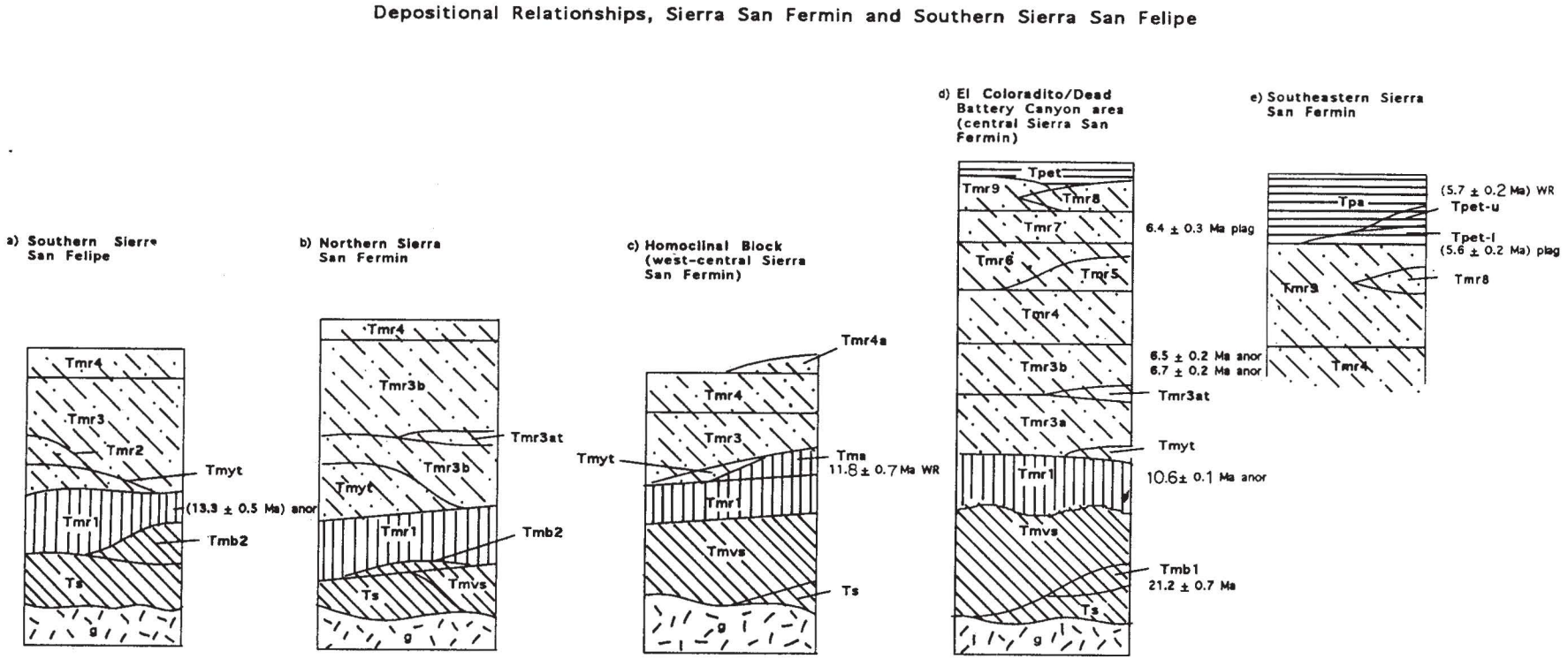

Fig. 3. Schematic stratigraphic columns summarizing depositional relationships in late Miocene–Pliocene sedimentary and volcanic units. Patterns follow group designations in Figure 2. Thicknesses are not to scale. Ages in parentheses are not considered reliable (see discussion in text).

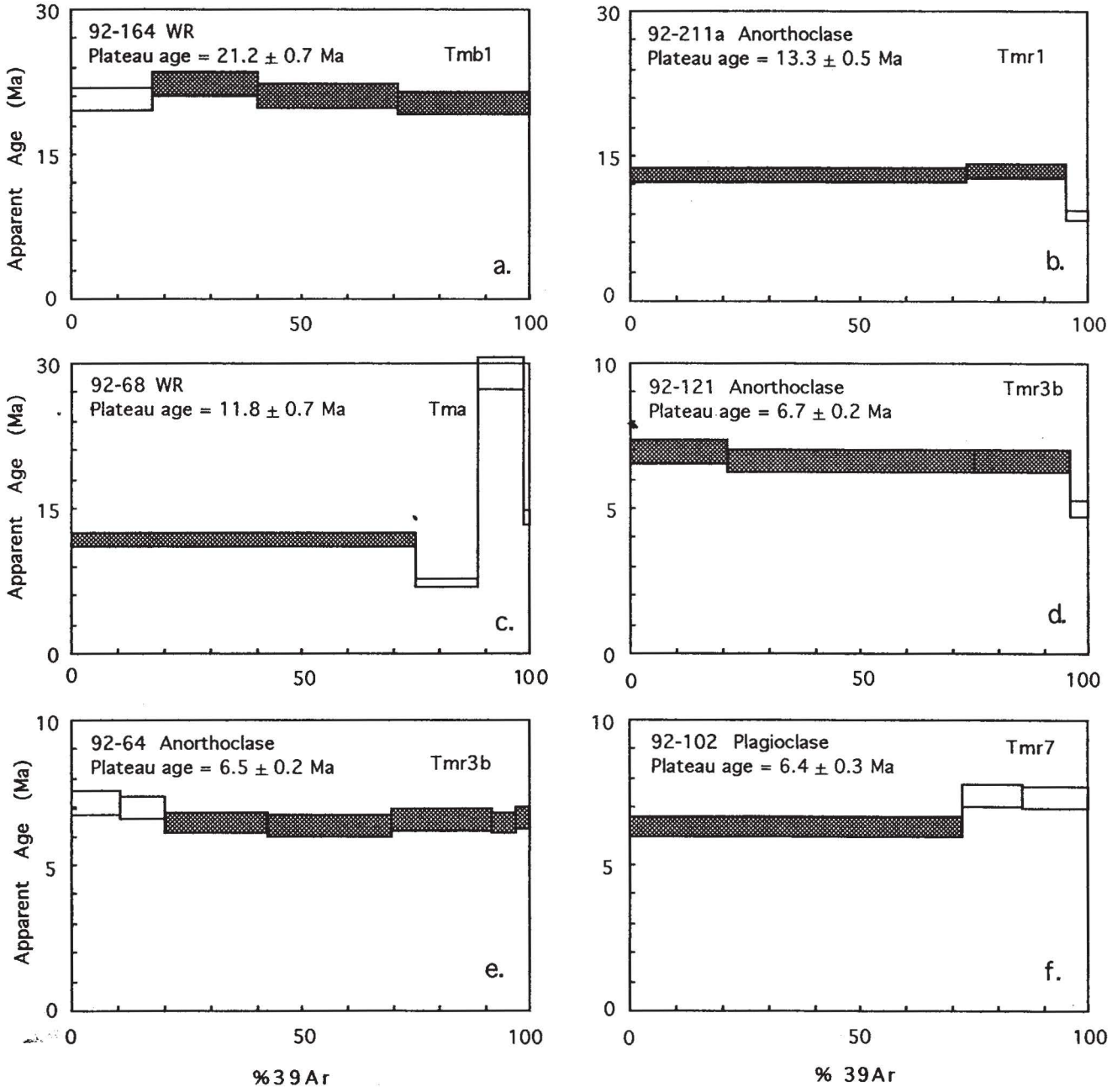

Fig. 4. $^{40}Ar/^{39}Ar$ age spectra for step–heated samples from Sierra San Fermín–Sierra San Felipe. All errors quoted at 2–σ. Shaded steps were used in calculation of plateau age. See Table 1 for MSWDs and $^{40}Ar/^{36}Ar$ ratios.

Tabular–bedded, cross–stratified sandstone overlies residual arkose and in most outcrops comprises all of Ts. Thickness of this facies ranges up to 100 m, varying due to erosional relief on basement rocks.

In the Bigfoot Mesa area of the Sierra San Felipe (C7–D7, Figure 2), tabular bedded sandstone grades upwards into clast–supported, imbricated cobble conglomerate. Very well–rounded dacite (?) clasts within the conglomerate may have been reworked from older deposits, as yet unidentified. Imbrications indicate a westward paleoflow direction (north-westward before vertical–axis block rotations are restored; Lewis, unpublished data). In the El Coloradito area (H14, I14, J14, K14, Figure 2), outcrops of dark red, cross–stratified arkosic sandstone and imbricated gravel are intercalated with basalt flows and cinders.

Although no fossil or plant remains were found in Ts, burrows approximately 20 cm in diameter occur locally in the buff–colored section (B7, Figure 2). A reddened zone at the top of the burrowed horizon, probably a paleosol, is overlain by conglomerate, in which abundant calcrete indicates prolonged pedogenesis.

In general, Ts resembles modern residual arkose and arkose presently forming in granitic hills and on proximal alluvial fans in the arid climate of this part of Baja

Table 1

Isotopic ages of selected volcanic units, Sierra San Fermín, northern Puertecitos Volcanic Province

(a) $^{40}Ar/^{39}Ar$ ages by step heating

Sample	Unit	Latitude (°N)	Longitude (°W)	Age(Ma)$_p$†	Age(Ma)$_i$*	MSWD	$(^{40}Ar/^{36}Ar)_0$	% ^{39}Ar§	Age(Ma)$_m$#	Age(Ma)$_s$£
92-164(wr)	Tmb1	30°30.70'	114°44.25'	**21.2 ± 0.7**	20.9 ± 1.2	1.9	306 ± 45	83	21.0 ± 0.2	
92-211a(anor)	Tmr1	30°41.65'	114°48.40'	13.3 ± 0.5#	**			95	13.0 ± 2.0	**10.6 ± 0.1**
92-68(wr)	Tma1	30°35.95'	114°45.30'	**11.8 ± 0.7**	11.8 ± 0.7	1.9	284 ± 52	76		
92-64(anor)	Tmr3b	30°35.50'	114°45.20'	**6.5 ± 0.2**	6.1 ± 0.3**	0.5	1008 ± 1158	80	7.1 ± 0.3	
92-121(anor)	Tmr3b	30°35.20'	114°46.25'	**6.7 ± 0.2**	7.0 ± 0.4	0.6	153 ± 103	96	6.7 ± 0.4	
92-102(plag)	Tmr7	30°33.30'	114°47.45'	**6.4 ± 0.3**	**			72	7.2 ± 0.4	
92-108(plag)	Tpet	30°30.75'	114°42.20'	**5.6 ± 0.2**	6.2 ± 0.3	0.2	215 ± 400	57	4.7 ± 0.8	~3
92-96(wr)	Tpa	30°31.30'	114°44.40'	5.7 ± 0.2††				71		**<3**

(b) $^{40}Ar/^{39}Ar$ ages by laser fusion

Sample	Unit	Latitude (°N)	Longitude (°W)	Age(Ma)$_i$*	MSWD	$(^{40}Ar/^{36}Ar)_0$	Age(Ma)$_m$#	n§§
92-116(anor)	Tmr1	30°41.65'	114°48.40'	9.1 ± 2.7**	3.0	648 ± 643	**10.6 ± 0.1**	10
92 - 110(plag)	?tuff	30°30.75'	114°42.20'	**8.2** ± 0.5	0.1	279 ± 70	8.1 ± 0.1	10

Abbreviations: plag, plagioclase; anor, anorthoclase; wr, whole rock.
Preferred ages in boldface.

†Plateau age.

*Intercept age. All steps used in calculation of ages except for step 3 of 92–68.

§Percentage of ^{39}Ar released in plateau increments.

#Weighted mean age.

£From stratigraphic constraints. See discussion in text.

††Low yields of radiogenic ^{40}Ar suggest this age is not realistic. See text for discussion.

**Points too clustered for well–constrained isochron.

§§Number of points fitted.

Decay constants as recommended by Steiger and Jaeger (1977).

California. Ts thus likely records weathering in place and short–distance transport and deposition in paleovalleys and proximal parts of alluvial fans that formed at the bases of prominent Tertiary hills and mountains.

The sandstones and conglomerates of Ts may be analogous to braided–stream deposits at the base of the middle Miocene Alverson Formation in the Salton Trough, California (Ruisaard, 1979). Tabular–bedded, cross–stratified sandstones accumulated there in a Platte–type braided stream system of broad, shallow channels on a westward–tilted pediment surface (Kerr, 1984). This system joined a northward–flowing, Donjek–type axial drainage system characterized by deep channels infilled with very coarse sand and gravel. By anology, the conglomeratic facies at Bigfoot mesa and El Coloradito may be remnants of westward–flowing, axial channel systems.

In the Sierra San Fermín, where Ts is intercalated with basalt flows (Tmb1) dated at 21.2 Ma, Ts is constrained to be early Miocene in age (Figure 3d). The basal part could be older, however. In the Cañon El Parral area of the Sierra San Felipe, buff–colored sandstone and conglomerate are overlain by 11 Ma welded tuff (e.g., B5–6, Figure 2) and, locally, older basalt (undated; E4–F4, Figure 2), making Ts there no younger than middle Miocene in age. These deposits are constrained to be post–Cretaceous by their content of batholithic and pre–batholithic clasts. In the absence of further age constraints they are classified here as Tertiary.

West of the Gulf Extensional Province (within northern Baja California), similar deposits of basal quartz–rich fluvial sandstone, which grade upwards into lower to middle Miocene volcanic rocks, are interpreted to be Oligocene (?) to middle Miocene in age (Dorsey and Burns, 1994). Until further stratigraphic and geochronologic work can be done, the relationship between these sandstones and Ts is uncertain.

Miocene Basalt 1 (Tmb1)

Basalt flows and bedded cinder deposits comprising Tmb1 crop out in the El Coloradito area (H14, I14, J14, K14, Figure 2), intercalated with fluvial sandstone Ts. The maximum exposed thickness of Tmb1 is about 20 m.

Miocene Rhyolite #3 (Tmr3b)

A nonwelded to densely welded pyroclastic flow (Tmr3b), rich in lithic fragments and crystals, occurs throughout the Sierra San Fermín and part of the southern Sierra San Felipe (Figure 3a–d). Where Tmr3b overlies tuff Tmr3a, the contact is conformable, but where Tmr3b overlies Miocene volcaniclastic rocks Tmvs, welded tuff Tmr1, or yellow–weathering tuffs Tmyt, the contact is disconformable or unconformable.

Wherever tuffs overlie 11 Ma Tmr1, Tmr3b is present and ranges in thickness from a few meters to about 120 m (Appendix C). The thickest densely welded outcrops, predominantly in the central part of the Sierra San Fermín, exhibit complex zonation due to welding, devitrification, and vapor phase crystallization. Fossil fumarolic mounds of silicified tuff occur locally at the top of Tmr3b .

Anorthoclase ($Ab_{65}An_2Or_{33}$) from two independent samples of Tmr3b (from localities 2 km apart) yielded plateau ages of 6.7 ± 0.2 (sample 92–121, basal vitrophyre) and 6.5 ± 0.2 Ma (sample 92–64, top tephra). These two ages are indistinguishable within uncertainties, suggesting that 6.5 or 6.7 ± 0.2 Ma are reliable ages for this unit.

Preservation of the cooling zonation in Tmr3b suggests that the overlying welded tuff, Tmr4, was deposited without major intervening erosion. The variations in thickness of Tmr3b (thickest in the central part of the Sierra San Fermín) parallel changes in the thickness of the underlying Tmr3a and the overlying welded tuff Tmr4. This, and conformity of all three units, suggests that they may be part of the same eruptive sequence. In at least one locality, however, considerable fracturing of the upper Tmr3b occurred prior to deposition of Tmr4 (F11, Figure 2). In these localities, Tmr4 fills cracks in Tmr3b, and blocks of Tmr3b are incorporated into the base of Tmr4. Fossil fumaroles were found in the same area, suggesting that degassing of Tmr3b might have played a role in this disruption of the Tmr3b.

Miocene Rhyolite #4 (Tmr4)

This densely welded vitric tuff crops out throughout the Sierra San Fermín, with the exception of the southeastern corner, and locally in the Cañon El Parral area of the southern Sierra San Felipe. Although Tmr4 is thin (<2 m) throughout much of the study area, in some localities it is considerably thicker (up to 50 m). The base of Tmr4, if unexposed, can be located by the concentration of fragments of brown frothy glass or brownish–black vitrophyre in the float, and thus constitutes a useful marker horizon.

Locally in the Sierra San Fermín, bedded tephra occurs at the base of Tmr4. Cross–bedding, lenticular bedding, channeling, and locally extensive disruption of bedding (bioturbation?) suggest that much of this section was reworked, although some beds are probably airfall units. The lowermost beds locally include boulders of Tmr3b as well as silicified boulders of tuff, possibly derived from fossil fumarolic mounds at the top of Tmr3b.

Where Tmr4 is thin, its base is typically orange ash, grading upwards into brown vitrophyre with flattened pumice and black fiamme (juvenile clasts?). The central part of the tuff is smooth, porcelainous devitrified tuff. The top is devitrified and vapor phase crystallized, partially welded to unwelded tuff. In some outcrops, lithophysal zones occur within the densely welded interior.

The thickest outcrops of Tmr4 (up to 50 m) are found in the east central and south central parts of the Sierra San Fermín (e.g., H11–I11 and H15, I14, Figure 2; Appendix C). Thickening of Tmr4 towards the south, paralleling thickness changes in underlying Tmr3a and Tmr3b, and a corresponding increase in the number of overlying, similar looking units (Tuffs of Dead Battery Canyon), suggest that the source for Tmr4 was to the south. Because thick sections of Tmr4 also occur near the eastern rangefront, an eastern source (presently beneath the coastal plain or within the Gulf of California) is possible. Tmr4 might have flowed westwards along paleocanyons or the margin of a caldera (e.g., H15, I14, Figure 2), accounting for the thick sections in these localities.

Locally, thin tuffs that overlie Tmr4, and closely resemble it in appearance, have been mapped with it. These units do not appear to be regional in extent. In some areas, variations in crystal, lithic and lapilli content suggest that Tmr4 as mapped comprises more than one ash flow.

Tmr4 was not dated, but stratigraphic relations allow the age of this tuff to be tightly constrained (Figure 3d). Over part of the Sierra San Fermín, symmetrical cooling zonation is preserved in the underlying Tmr3b (6.5 Ma) tuff, and no significant erosional unconformity is developed between the two units. Similar relations to the west in correlative units of southern Valle Chico suggest that Tmr4 and Tmr3b are close in age (Stock, 1989). The 6.4 ± 0.3 Ma age of an overlying tuff, Tmr7, makes Tmr4 about 6.5 Ma as well.

Miocene Rhyolite #4a (Tmr4a)

Near the western rangefront of the Sierra San Fermín, a moderately crystal–rich tuff (~3 m thick) overlies Tmr4 (C14–C15, Figure 2), which does not appear to have been eroded prior to deposition of the overlying unit. Tmr4a might be correlative with one of the Tuffs of Dead Battery Canyon described below, perhaps Tmr5.

The Tuffs of Dead Battery Canyon

Miocene Rhyolite #5 (Tmr5)

Tmr5 occurs in the Dead Battery Canyon/El Coloradito area (e.g., F14–G14, Figure 2; Appendix C). Less continuous than the overlying Tmr6, Tmr5 was probably deposited on a surface of modest topographic relief in welded tuff Tmr4. Tmr5 can be distinguished readily from the

more crystal–rich welded tuff that overlies it (Tmr6), where the two are found together.

Miocene Rhyolite #6 (Tmr6)

The principal outcrops of welded tuff Tmr6 are the Dead Battery Canyon and El Coloradito areas (e.g., F14–G14 and I14–J14, Figure 2; Appendix C). Characteristically, Tmr6 lacks a basal vitrophyre. Its central zone is brown, partially welded, and very rich in somewhat flattened and vapor–phase crystallized pumice blocks up to 25 cm long and 10 cm wide. The upper unwelded zone, variably preserved, is extensively vapor–phase devitrified. In some localities, blocks of upper Tmr6 are incorporated into overlying tephra beds.

Whereas Tmr6 and Tmr7 appear conformable in the Dead Battery Canyon area, a conspicuous unconformity is developed on top of Tmr6 in the El Coloradito area (I14–J14, Figure 2). Tmr6 there was tilted about 5° westwards, and much of it was eroded, prior to deposition of Tmr7. These relations, and the occurrence of blocks of rhyolite in the upper part of Tmr6, suggest faulting and block tilting during or just after eruption of Tmr6, perhaps near the edge of a caldera.

Miocene Rhyolite #7 (Tmr7)

Miocene rhyolite Tmr6 is overlain near Dead Battery Canyon (F14, Figure 2) by about 8 m of bedded airfall tephra and a sequence of 5 unwelded pumice flows (Appendix C). Many of these units are present only locally, and range in thickness from <1 m to about 9 m. All 5 pumice flows are similar in appearance, typically unwelded and brown–weathering with white or pink silicified bases.

All of the units of Tmr7 contain gray, feldspar–rich pumice and dark gray or black nonvesiculated glass. Flow foliated, dark purplish–black rhyolite lithic fragments increase in volume upsection. The similarity of these units one to another and the upwards increase in rhyolite lithic inclusions suggests that they were all erupted in a very short time and that they represent an explosive eruptive phase preceding the effusion of the overlying rhyolite flows.

$^{40}Ar/^{39}Ar$ ages were obtained on rare, microperthitic feldspar ($Ab_{73}An_{19}Or_7$; oligoclase) separated from gray, vesiculated lapilli contained within the second brown–weathering tuff (sample 92–102). Step heating gave a plateau age of 6.4 ± 0.3 Ma, consistent with the stratigraphic position of this tuff upsection of Tmr3b. Because this age is concordant with ages for Tmr3b, Tmr7 was likely deposited shortly after Tmr3b.

Miocene Rhyolite #8 (Tmr8)

Miocene rhyolite Tmr8 is a compound cooling unit, many tens of meters thick, of lithic–rich welded tuff (Lewis, 1994). The contacts between individual eruptive units cannot be readily mapped because of welding, but outcrops of Tmr8 have a banded appearance due to subtle variations in lithic content and degree of compaction and/or welding.

This tuff crops out in the El Coloradito area, where it is both underlain and overlain by rhyolite flows Tmr9 (I14–J14, Figure 2). Its appearance and association with rhyolite flows suggests that it is a near–vent airfall or ash-flow unit. It is also found in shutter ridges (created by Pliocene to Recent sinistral faulting) at the mouths of canyons east of Dead Battery Canyon, where it is underlain by a thick unwelded pumice flow of Tmr7 (H15, I15, Figure 2). Though Tmr8 was not dated in this study, it is constrained to be younger than the 6.4 Ma Tmr7 (Figure 3d).

Tmr8 was not recognized in the Dead Battery Canyon area, but it might be the same unit as the breccia and ash agglomerate that underlies Tmr9 there (Appendix C). This suggests that the thicker, densely welded outcrops to the east are nearer to the source.

Undifferentiated Miocene Rhyolites (Tmr9)

Tmr9 consists of undifferentiated rhyolite flows, local ash flow tuffs, and rhyolite agglomerates that comprise coalesced domes and coulees in the southeastern Sierra San Fermín (Figure 2). This part of the Sierra San Fermín is thus an area of numerous rhyolite vents. These domes may be located within a caldera ≥ 6 Ma in age (see below).

Many of the flows in Tmr9 exhibit the classic stratigraphy of a rhyolite flow, including a basal block and ash layer, welded rhyolite breccia, and a 20– to 200–m thick central zone of flow banded, devitrified stony rhyolite. This central part in some flows contains extremely contorted flow foliations, brecciated slabs of foliated rhyolite welded together in masses, and ramp structures indicative of primary deformation during deposition of viscous rhyolite. Some flows contain large percentages of pumice and lithic lapilli, especially near their bases. Flows of Tmr9 overlie, with angular unconformity, welded tuff Tmr4 and interfinger with tuffs of the Dead Battery Canyon sequence (Tmr5, Tmr6, and Tmr7) and welded tuffs Tmr8.

Locally in the southeasternmost corner of the Sierra San Fermín, Tmr9 includes thin, near–source tuffs. Plagioclase ($Ab_{66}An_{30}Or_3$; andesine) from one of these tuffs (sample 92–110) gave an intercept age of 8.2 ± 0.5 Ma and a weighted mean age of 8.1 ± 0.1 Ma (see discussion of significance of these ages below).

PLIOCENE ROCKS

Group 4 (<3 Ma volcanic rocks)

Tuffs of Mesa El Tábano (Tpet)

Densely welded Tuffs of Mesa El Tábano (Tpet) crop out discontinuously in the southern Sierra San Fermín, and have not been recognized north of the Dead Battery Canyon area (Figure 2; Lewis, 1994). Their principal outcrop area is Mesa El Tábano (Figure 1) and further south, along the

east side of the Puertecitos Volcanic Province. Because of their broad areal distribution and characteristic phenocryst assemblage, the Tuffs of Mesa El Tábano are important marker units for correlations, structural analysis, and paleomagnetic rotations along a 25–km stretch of coast from the Sierra San Fermín south (e.g. Stock *et al.*, 1991; Martín Barajas and Stock, 1993; Melbourne *et al.*, 1993). The number of units and their thicknesses increase southwards, suggesting that the source for the Tuffs of Mesa El Tábano is to the south (Stock *et al.*, 1991).

Near Dead Battery Canyon (F14–15, Figure 2), two units make up the Tuffs of Mesa El Tábano. The lowermost unit is a distinctive brown airfall tephra. The upper unit is a thin (<2 m), densely welded ash flow tuff. These units overlie rhyolite flows Tmr9 and underlie reworked tephra, alluvial units, and lacustrine or marine mudstones (Lewis, 1994).

Two conformable ash flow tuffs with lithologic characteristics similar to Tpet in the Dead Battery Canyon area occur in the southeasternmost Sierra San Fermín (K17, Figure 2; Figure 3e). The thinness of these tuffs, their densely welded character, and the occurrence of two clinopyroxenes (augite and diopside?) suggest that they were probably very hot when erupted (e.g. Hildreth, 1979). Similarities in stratigraphic position, lithologic characteristics, and vectors of magnetization (Lewis, 1993; Melbourne *et al.*, 1993) suggest that these tuffs correlate with the Tuffs of Mesa El Tábano (Stock *et al.*, 1991; Martín Barajas *et al.*, 1993) between Arroyo Matomí and Puertecitos (Figure 1).

A plateau age of 5.6 ± 0.2 Ma was obtained from plagioclase ($Ab_{62}An_{36}Or_2$; andesine) from the lower tuff (sample 92–108). This age is discordant with the ~3 Ma ages obtained on Tuffs of Mesa El Tábano in adjacent areas (Sommer and Garcia, 1970; Martín–Barajas *et al.*, 1995; see discussion below). Further geochronologic work should be done to confirm whether the two tuffs are actually older than 3 Ma in age.

Pliocene Andesite (Tpa)

A sequence of porphyritic, pyroxene–bearing andesite flows and monolithologic debris flows and breccias, reaching thicknesses of several hundred meters, caps the highest elevations of the southeastern Sierra San Fermín (vicinity J16, Figure 2; Appendix C). Outcrop characteristics suggest that the debris flows and breccias were locally derived from flows of Tpa on steep flanks of Tpa vents.

Beneath Tpa in some localities is epiclastic, crystal–rich volcanic sandstone up to 2 m thick. These deposits are tabular bedded and distinctly cross–laminated, suggesting that they are dilute–streamflow alluvial deposits. Because of their similarity in crystal content, these deposits were mapped with Tpa.

A whole rock sample of Tpa yielded a plateau age of 5.7 ± 0.2 Ma (sample 92–96), but the low yields of radiogenic ^{40}Ar gas (≤ 13%) in each increment make this age unreliable. A 5.7 Ma age is also inconsistent with stratigraphic relationships; on the north side of Arroyo Matomí (Figure 1) and in the southeastern Sierra San Fermín, flows and breccias of this andesite complex [unit Mb6 of Stock *et al.* (1991); Figure 5] overlie the Tuffs of Mesa El Tábano. Isotopic ages, discussed below, on the Tuffs of Mesa El Tábano constrain Tpa to be younger than 3 Ma.

Group 5 (sedimentary rocks)

This group includes terrestrial and marine sedimentary rocks which unconformably overlie late Miocene volcanic rocks. The terrestrial part of the section will be described here, and the marine part in a subsequent paper.

Pliocene (?) Sedimentary Rocks (Ps)

This unit includes Pliocene (?) conglomerate, sandstone, and mudstone overlying late Miocene tuffs and rhyolite flows. The two principal outcrops of Ps are located in structural embayments in the western range front of the Sierra San Fermín, at Ironwood Canyon and near the mouth of Dead Battery Canyon (G8–H8, E15–F15, Figure 2). The base of these sections consists of thinly bedded pinkish–brown mudstones with a large component of volcanic ash and lenses of very fine grained sandstone, silty mudstone, and pumice and lithic lapilli conglomerate (Lewis, 1994). These fine grained deposits grade upwards into coarse volcanic conglomerates with minor sandstone.

The sediments that comprise Ps were deposited in actively subsiding, fault–bounded basins. Ps represents lacustrine (marine?) deposits at the centers of internally drained basins and marginal colluvial and alluvial fan deposits. The upwards transition from lacustrine deposits to coarse alluvial deposits suggests that fluvial conglomerates ultimately prograded out from basin margins across former lakes.

Throughout the area, Pliocene sedimentary rocks are tectonically deformed, dipping as much as 35° in some localities, and highly dissected. Where Ps overlies the unwelded top of the 6 Ma tuff Tmr4, deposition may have begun in latest Miocene time. Ps may be partly coeval with marine deposits at the eastern range front of the Sierra San Fermín (Figure 2).

CORRELATIONS WITH VOLCANIC ROCKS FROM ADJACENT AREAS

Southern Valle Chico Area

Many of the units present within this study area are also present to the west in the southern Valle Chico area [Figures 1 (area S93) and 5; Stock and Hodges, 1989; Stock, 1993]. With some exceptions, the southern Valle Chico section is the same as that in the Sierra San Fermín. Correlative packages/units [using the unit designations of Stock (1989)] include, from oldest to youngest: conglomerate, sandstone and tuff with local basalt bodies (Tmvs), capped by welded tuff (Tmr1); andesite to rhyolite flows

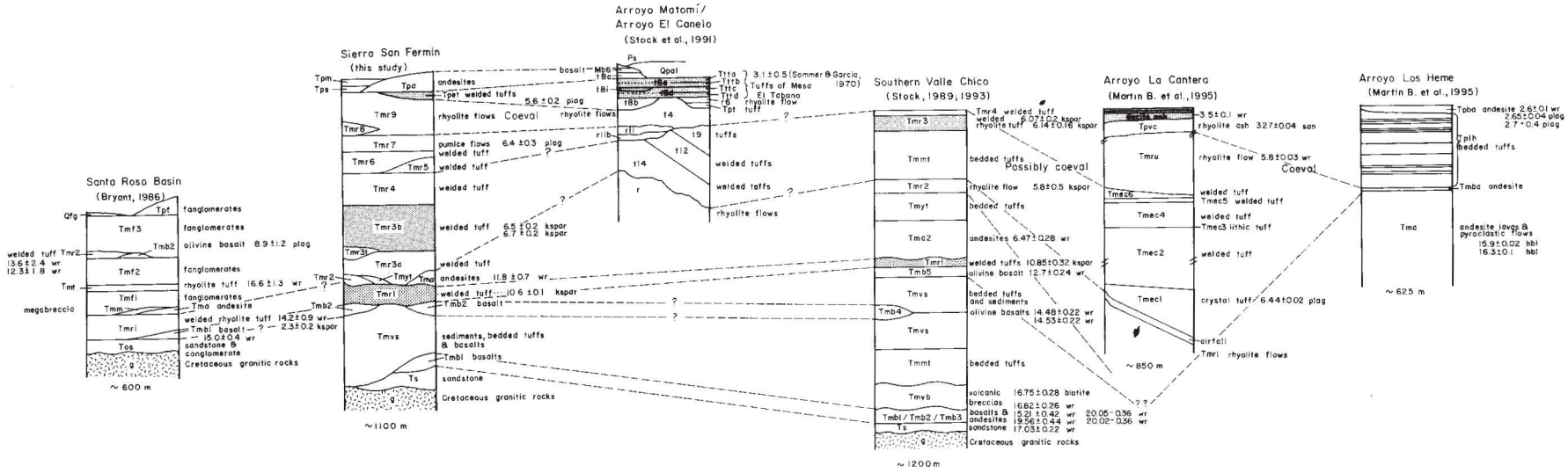

Fig. 5. Stratigraphic correlations between the Sierra San Fermín and adjacent areas. Correlations with sections to the south and west suggest the regional extent of many of the late Miocene/Pliocene ash flow tuffs. The late Miocene volcanic section in the Sierra San Fermín comprises many of the same units as the southern Valle Chico section (Stock, 1989; Stock, 1993). The Pliocene volcanic section contains some of the same units that are found in Arroyo Matomí/Arroyo El Canelo and Arroyo La Cantera (Stock *et al.*, 1991; Martín Barajas and Stock, 1993; Martín–Barajas *et al.*, 1995). Correlations between the Sierra San Fermín and the Sierra Santa Rosa, to the north, are as yet uncertain.

east side of the Puertecitos Volcanic Province. Because of their broad areal distribution and characteristic phenocryst assemblage, the Tuffs of Mesa El Tábano are important marker units for correlations, structural analysis, and paleomagnetic rotations along a 25–km stretch of coast from the Sierra San Fermín south (e.g. Stock *et al.*, 1991; Martín Barajas and Stock, 1993; Melbourne *et al.*, 1993). The number of units and their thicknesses increase southwards, suggesting that the source for the Tuffs of Mesa El Tábano is to the south (Stock *et al.*, 1991).

Near Dead Battery Canyon (F14–15, Figure 2), two units make up the Tuffs of Mesa El Tábano. The lowermost unit is a distinctive brown airfall tephra. The upper unit is a thin (<2 m), densely welded ash flow tuff. These units overlie rhyolite flows Tmr9 and underlie reworked tephra, alluvial units, and lacustrine or marine mudstones (Lewis, 1994).

Two conformable ash flow tuffs with lithologic characteristics similar to Tpet in the Dead Battery Canyon area occur in the southeasternmost Sierra San Fermín (K17, Figure 2; Figure 3e). The thinness of these tuffs, their densely welded character, and the occurrence of two clinopyroxenes (augite and diopside?) suggest that they were probably very hot when erupted (e.g. Hildreth, 1979). Similarities in stratigraphic position, lithologic characteristics, and vectors of magnetization (Lewis, 1993; Melbourne *et al.*, 1993) suggest that these tuffs correlate with the Tuffs of Mesa El Tábano (Stock *et al.*, 1991; Martín Barajas *et al.*, 1993) between Arroyo Matomí and Puertecitos (Figure 1).

A plateau age of 5.6 ± 0.2 Ma was obtained from plagioclase ($Ab_{62}An_{36}Or_2$; andesine) from the lower tuff (sample 92–108). This age is discordant with the ~3 Ma ages obtained on Tuffs of Mesa El Tábano in adjacent areas (Sommer and Garcia, 1970; Martín–Barajas *et al.*, 1995; see discussion below). Further geochronologic work should be done to confirm whether the two tuffs are actually older than 3 Ma in age.

Pliocene Andesite (Tpa)

A sequence of porphyritic, pyroxene–bearing andesite flows and monolithologic debris flows and breccias, reaching thicknesses of several hundred meters, caps the highest elevations of the southeastern Sierra San Fermín (vicinity J16, Figure 2; Appendix C). Outcrop characteristics suggest that the debris flows and breccias were locally derived from flows of Tpa on steep flanks of Tpa vents.

Beneath Tpa in some localities is epiclastic, crystal–rich volcanic sandstone up to 2 m thick. These deposits are tabular bedded and distinctly cross–laminated, suggesting that they are dilute–streamflow alluvial deposits. Because of their similarity in crystal content, these deposits were mapped with Tpa.

A whole rock sample of Tpa yielded a plateau age of 5.7 ± 0.2 Ma (sample 92–96), but the low yields of radiogenic ^{40}Ar gas (≤ 13%) in each increment make this age unreliable. A 5.7 Ma age is also inconsistent with stratigraphic relationships; on the north side of Arroyo Matomí (Figure 1) and in the southeastern Sierra San Fermín, flows and breccias of this andesite complex [unit Mb6 of Stock *et al.* (1991); Figure 5] overlie the Tuffs of Mesa El Tábano. Isotopic ages, discussed below, on the Tuffs of Mesa El Tábano constrain Tpa to be younger than 3 Ma.

Group 5 (sedimentary rocks)

This group includes terrestrial and marine sedimentary rocks which unconformably overlie late Miocene volcanic rocks. The terrestrial part of the section will be described here, and the marine part in a subsequent paper.

Pliocene (?) Sedimentary Rocks (Ps)

This unit includes Pliocene (?) conglomerate, sandstone, and mudstone overlying late Miocene tuffs and rhyolite flows. The two principal outcrops of Ps are located in structural embayments in the western range front of the Sierra San Fermín, at Ironwood Canyon and near the mouth of Dead Battery Canyon (G8–H8, E15–F15, Figure 2). The base of these sections consists of thinly bedded pinkish–brown mudstones with a large component of volcanic ash and lenses of very fine grained sandstone, silty mudstone, and pumice and lithic lapilli conglomerate (Lewis, 1994). These fine grained deposits grade upwards into coarse volcanic conglomerates with minor sandstone.

The sediments that comprise Ps were deposited in actively subsiding, fault–bounded basins. Ps represents lacustrine (marine?) deposits at the centers of internally drained basins and marginal colluvial and alluvial fan deposits. The upwards transition from lacustrine deposits to coarse alluvial deposits suggests that fluvial conglomerates ultimately prograded out from basin margins across former lakes.

Throughout the area, Pliocene sedimentary rocks are tectonically deformed, dipping as much as 35° in some localities, and highly dissected. Where Ps overlies the unwelded top of the 6 Ma tuff Tmr4, deposition may have begun in latest Miocene time. Ps may be partly coeval with marine deposits at the eastern range front of the Sierra San Fermín (Figure 2).

CORRELATIONS WITH VOLCANIC ROCKS FROM ADJACENT AREAS

Southern Valle Chico Area

Many of the units present within this study area are also present to the west in the southern Valle Chico area [Figures 1 (area S93) and 5; Stock and Hodges, 1989; Stock, 1993]. With some exceptions, the southern Valle Chico section is the same as that in the Sierra San Fermín. Correlative packages/units [using the unit designations of Stock (1989)] include, from oldest to youngest: conglomerate, sandstone and tuff with local basalt bodies (Tmvs), capped by welded tuff (Tmr1); andesite to rhyolite flows

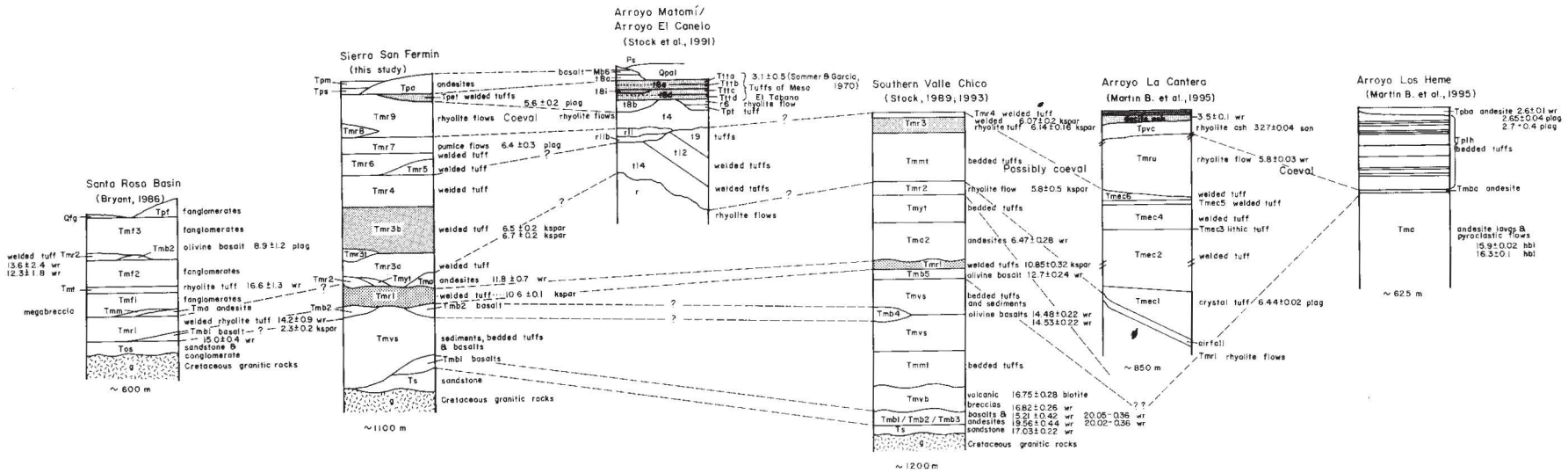

Fig. 5. Stratigraphic correlations between the Sierra San Fermín and adjacent areas. Correlations with sections to the south and west suggest the regional extent of many of the late Miocene/Pliocene ash flow tuffs. The late Miocene volcanic section in the Sierra San Fermín comprises many of the same units as the southern Valle Chico section (Stock, 1989; Stock, 1993). The Pliocene volcanic section contains some of the same units that are found in Arroyo Matomí/Arroyo El Canelo and Arroyo La Cantera (Stock *et al.*, 1991; Martín Barajas and Stock, 1993; Martín–Barajas *et al.*, 1995). Correlations between the Sierra San Fermín and the Sierra Santa Rosa, to the north, are as yet uncertain.

and domes (Tma2); and rhyolite glass flows (Tmr2), bedded tuffs and pyroclastic flows (Tmyt, Tmmt and Tmr3), capped by a densely welded tuff (Tmr4).

The oldest ages reported for southern Valle Chico (20.05 ± 0.36, 20.02 ± 0.36, and 19.56 ± 0.42 Ma 2–σ K–Ar whole rock ages on basalts) are concordant with the 21.2 Ma age of olivine basalt in the Sierra San Fermín, indicating coeval basaltic volcanism in both areas in middle Miocene time.

The 10.85 ± 0.32 Ma age on Tmr1 welded rhyolite tuff agrees with the age of 10.6 ± 0.1 Ma determined on the same tuff in the Sierra San Fermín. Paleomagnetic results from outcrops of Tmr1 in southern Valle Chico and Sierra San Fermín corroborate this correlation (Lewis, unpublished data).

Hornblende andesite (Tma2) in southern Valle Chico occupies a similar stratigraphic position as hornblende andesite (Tma) from the Sierra San Fermín. The 6.47 ± 0.28 Ma age on Tma2 (Stock, 1989) does not agree with the 11.8 ± 0.7 Ma whole rock age from the Sierra San Fermín, indicating that andesitic vents in this stratigraphic position may vary in age.

The 6.07 ± 0.20 and 6.14 ± 0.16 Ma ages of Tmr3 (Stock, 1989) are concordant with the 6.5 ± 0.2 Ma age obtained on the same tuff (Tmr3b) from the Sierra San Fermín. In southern Valle Chico, Tmr3 is underlain by a package of unwelded, crystal–lithic tuffs, the Tuffs of Matomí (Tmmt). The uppermost of these tuffs correlates lithologically and paleomagnetically with Tmr3a in the Sierra San Fermín (Lewis, unpublished data).

The mesa–capping tuff in the southern Valle Chico area, Tmr4, correlates lithologically and paleomagnetically with the mesa–capping tuff in the Sierra San Fermín (Lewis, unpublished data). This unit was not dated in either study.

No specific correlative units in the southern Valle Chico area have been identified for the Tuffs of Dead Battery Canyon in the Sierra San Fermín. This package might correlate with t2, t4 and t3 located in the Mpru hills southeast of Mesa Cuadrada (Stock, 1989; Stock *et al.*, 1991), which were deposited after significant normal faulting had occurred on the eastern front of the Sierra San Felipe. These correlations should be investigated further.

Arroyo Matomí/Arroyo El Canelo

A thick section of rhyolite flows and ignimbrites crops out in the Arroyo Matomí/Arroyo El Canelo area [Figures 1 (area M95) and 5] south of the Sierra San Fermín. Three principal units are exposed in this area: the Tuffs of El Canelo, rhyolite or dacite flows and associated tephra, and the Tuffs of Mesa El Tábano, as well as submarine equivalents of some of the ignimbrites (Stock *et al.*, 1991; Martín Barajas and Stock, 1993; Martín–Barajas *et al.*, 1995).

The Tuffs of El Canelo (Tmec) are comprised of three ignimbrites: (1) t14, an unwelded, lithic lapilli tuff with rare plagioclase phenocrysts, (2) t12, a densely welded, crystal– and lithic–rich tuff with numerous partial cooling breaks, and (3) t9, a non– to partially welded, lithic and pumice lapilli tuff containing large landslide blocks (Stock *et al.*, 1991; Stock, 1994, personal communication). Tmec is pervasively faulted by closely–spaced domino faults and tilted 50–70° towards the west-southwest (Stock *et al.*, 1991; Martín Barajas and Stock, 1993; Martín–Barajas *et al.*, 1995). Units t12 and t9 may constitute intracaldera fill or at least proximal ignimbrite facies.

Late Miocene K–Ar ages reported from volcanic units in Arroyo El Canelo (Sommer and Garcia, 1970; Gastil *et al.*, 1975; Gastil *et al.*, 1979), compared with the stratigraphy of Stock *et al.* (1991), suggest that the Tuffs of El Canelo are 7–9 Ma and the overlying rhyolite flows 5.9 ± 0.2 Ma. If the Tuffs of El Canelo really are 7–9 Ma in age (see discussion below), then they may be correlative with tuffs, including one dated in this study at 8.2 ± 0.5 Ma, which crop out in the southeastern Sierra San Fermín. An ~ 9.3 Ma dacite (?) flow southeast of Mesa Cuadrada may also be related to this sequence [Figure 1 (area N); E. Nagy, personal communication].

Stratigraphic evidence suggests limited volcanism between 11 and 6 Ma, but the evidence for a regional hiatus in deposition is equivocal. The scarcity of units between 11 and 6 Ma in age in the study area may have resulted from locally high topography in the Sierra San Fermín bordered by a fault–controlled basin or caldera in the vicinity of Arroyo Matomí.

The flat–lying Tuffs of Mesa El Tábano (Tpet) comprise a sequence of four ignimbrites and local airfall tephra. The lowermost two of these ignimbrites are poorly welded, whereas the upper two are densely welded. All the tuffs in this sequence include phenocrysts of feldspar (typically plagioclase), clinopyroxene, and olivine. The uppermost tuff has been dated at 3.1 ± 0.5 Ma [1–σ K–Ar; Sommer and Garcia, 1970].

The welded tuff and associated airfall tephra that comprise the Tuffs of Mesa El Tábano in the Dead Battery Canyon area may be the same as Tpet sub–unit Tttc of Stock *et al.* (1991), the second ignimbrite from the bottom of the Mesa El Tábano sequence (Figure 5). This correlation is based on similar phenocryst assemblages, in particular the presence of hornblende, in both units. Under– and overlying tuffs have been dated at 3.27 ± 0.04 and 3.08 ± 0.04 Ma in age (Martín–Barajas *et al.*, 1995), suggesting an intermediate age for Tpet of the present study.

Puertecitos Region

The rocks of the Puertecitos region have been divided into three groups: (1) andesitic and dacitic rocks corresponding to the early and middle Miocene andesitic arc, (2) rhyolite domes and flows, a sequence of ash flow tuffs (Tuffs of El Canelo), bounded above and below by rhyolite flows, and local andesite flows, and (3) a series of ig-

nimbrites (Tuff of Valle Curbina, Tuffs of Mesa El Tábano, and Tuffs of Los Heme) overlain locally by andesite flows [Figures 1 (area M95) and 5; Martín–Barajas *et al.*, 1995]. Of principal interest to this study are the Tuffs of El Canelo.

In Arroyo La Cantera, the Tuffs of El Canelo [abbreviated Tmec here after Stock *et al.* (1991), although Martín–Barajas *et al.* (1995) designate this sequence "Tmc"] consist of six cooling units with a cumulative thickness of 300 m. This sequence erupted between 6.4 and 5.8 Ma. Anorthoclase from the basal tuff, which directly overlies rhyolite flows, was dated at 6.44 ± 0.02 Ma. Unit 5 of the Arroyo La Cantera section has been correlated with the densely welded, compound cooling unit t12 in the Arroyo Matomí/ Arroyo El Canelo area, although t12 may include more than just unit 5. This correlation calls into question the 7–9 Ma ages reported from tuffs in Arroyo El Canelo (Sommer and Garcia, 1970; Gastil *et al.*, 1975; Gastil *et al.*, 1979).

It is possible that the Arroyo La Cantera section correlates with the Tuffs of Dead Battery Canyon, and the older units Tmr3a, Tmr3b, and Tmr4 in the Sierra San Fermín (Figure 5). Martín–Barajas *et al.*'s (1995) 6.44 ± 0.02 Ma age on unit 1 in the La Cantera section is concordant with the 6.5 ± 0.2 Ma age for Tmr3b and with the 6.4 ± 0.3 Ma age for Tmr7 in this study. Because Martín *et al.*'s unit 1 is crystal–rich and contains potassic feldspar, it probably is not the same as Tmr4–Tmr7. It could, however, be the same as either Tmr3a or Tmr3b of the present study. The progression from crystal–rich to crystal–poor tuffs and from a phenocryst assemblage rich in potassic feldspar to one composed of two pyroxenes and plagioclase is similar to that seen within the combined Tmr3a–Tmr8 sequence in the present study.

The phenocryst assemblage of the Tuffs of El Canelo in Arroyo Matomí/Arroyo El Canelo is consistent with that of the ~6.4 Ma tuffs Tmr4–Tmr8 of the present study but not with that of the slightly older Tmr3a or Tmr3b. As the base of Tmec is not exposed, it is not known whether units correlative with Tmr3a or Tmr3b lie underneath. Thickening of Tmr4 towards outcrops of Tmec and pervasive faulting of Tmr4 similar to that seen in Tmec are consistent with these being correlative units. Perhaps t12 is a compound cooling unit comprised of plagioclase– and pyroxene–bearing welded tuffs Tmr4–Tmr8, one of which may correlate with unit 5 of Arroyo La Cantera.

The Tuffs of El Canelo, in this scenario, may be intracaldera facies in the El Canelo area and outflow facies in the Sierra San Fermín, southern Sierra San Felipe, southern Valle Chico, and Puertecitos area. The major east-northeast–striking structures in the Dead Battery Canyon/ El Coloradito area (Figure 2) may have developed at the northern edge of a caldera associated with eruption of the oldest units in the 6 Ma Arroyo La Cantera and Sierra San Fermín sequences. The anomalous thicknesses of Tmr3a and Tmr3b in the Dead Battery Canyon/El Coloradito area may have resulted from partial ponding against this structure. An inner caldera may have developed as Tmr4–Tmr8 were erupted, ponding the near–vent facies (Tmec) in the Arroyo El Canelo area. Continued growth of the El Coloradito structure during the 6 Ma eruptive cycle might explain the great thickness of Tmr4 there and the confinement of Tmr5–Tmr9 to the area south of Dead Battery Canyon, the lack of basement outcrops south of the Dead Battery area, and the location of 6 and 3 Ma rhyolite and andesite eruptive centers in the southeastern Sierra San Fermín and Arroyo Matomí area. It should be noted that none of the correlations discussed here have been confirmed, and further work is needed to determine exactly where Tmec fits into the late Miocene–Pliocene volcanic section, especially in light of sparse, but significant, 7–9 Ma ages from this area.

Santa Rosa Basin

This area lies 20 km north-northwest of the northern end of the map area [Figure 1 (area B86)]. Volcanic rocks interbedded with sedimentary rocks have yielded K–Ar ages ranging from 16 to 9 Ma (Figure 5; Gastil *et al.*, 1975; Gastil *et al.*, 1979; Bryant, 1986). Gastil *et al.* (1979) reported a whole–rock K–Ar age of 14.2 ± 0.9 Ma on the basal vitrophyre of the lowest tuff in the Santa Rosa Basin. The ages of rhyolite tuffs higher in the section are not very well constrained. Because of stratigraphic and geochronologic similarities between the sections in the present study area and in the Sierra Santa Rosa, as well as their physical proximity, further work should be done to determine correlations.

Isla Tiburón

The stratigraphic section found on Isla Tiburón (Figure 1) and the adjacent coast of Sonora is important to studies of early Gulf rifting. Distinctive Permian, fusilinid–bearing carbonate clasts in fluvial conglomerate provide a tie point across the Gulf between coastal Sonora and the Sierra Santa Rosa (Figure 1; Gastil *et al.*, 1973; Gastil *et al.*, 1979; Bryant, 1986). Correlation of these conglomerates suggests a 300–km dextral displacement of Baja California relative to mainland Mexico. Gastil *et al.*'s (1973) restoration of this offset juxtaposes Isla Tiburón and adjacent coastal Sonora to a position near the Sierra San Fermín, suggesting the sections may be in part correlative and may provide a late Miocene/Pliocene tie–point across the Gulf.

Further work is necessary to determine correlations between these two sections, but some preliminary conclusions may be drawn here. At the southwestern end of Isla Tiburón, a thick section of marine conglomerate overlies the dominantly andesitic section (Gastil *et al.*, 1973; Gastil *et al.*, 1974; Gastil and Krummenacher, 1977; Weaver, 1981; Smith *et al.*, 1985; Neuhaus, 1989). This is the oldest known exposure of marine rocks in the Gulf (Gastil *et al.*, 1979; Smith *et al.*, 1985; Neuhaus, 1989). Within the marine section is a volcanic debris flow dated at 12.9 ± 0.4 Ma (Smith *et al.*, 1985). No marine rocks of this age have been identified in the present study. However, the marine section on Isla Tiburón is overlain unconformably by an ash flow tuff dated at 11.2 ± 1.3 Ma (Gastil and Krummenacher, 1977), concordant with the 10.6 ± 0.1 Ma

isotopic age obtained in this study for Tmr1. These could be the same tuff.

The 11.2 Ma Isla Tiburón tuff is the basal unit in a sequence of dominantly rhyolitic and dacitic units, perhaps correlative with the 11–6 Ma section of this study. On Isla Tiburón, this sequence is faulted and tilted and overlain unconformably by flat–lying to slightly tilted, but largely unfaulted, rhyolites and dacites. No ages have been obtained on these youngest units. Their stratigraphic position and relative lack of deformation suggest that they might be correlative with the Tuffs of Mesa El Tábano. Further study is necessary to test these correlations.

CONCLUSIONS

The Sierra San Fermín is a site of late Miocene/Pliocene volcanism largely related to extensional faulting within the boundary zone between the Pacific and North America plates. The Sierra San Fermín is located within part of the early to middle Miocene, subduction–related volcanic arc that extended the length of the Baja California peninsula. The study area straddles two major, post–subduction vent areas, an 11 Ma vent to the north and a 60 km^2 area of ~6 Ma (and possibly 8 Ma) intracaldera fill, including ash flow tuffs and coalesced rhyolite domes to the south. Depositional relationships within the late Miocene section suggest that extension began in this area between 11 and 6 Ma. Much of the topography on the steep eastern escarpment of the Sierra San Felipe formed sometime after 6 Ma.

The post–batholithic strata of the Sierra San Fermín and the northern Sierra San Felipe can be divided into 5 major sequences. These are, from oldest to youngest: Group 1: sandstones (Ts), basalt flows, andesite breccias, and conglomerate capped in some places by more basalt flows (Tmvs); Group 2: an 11 Ma welded rhyolitic tuff (Tmr1) and andesites (Tma); Group 3: epiclastic volcanic rocks, ignimbrites and rhyolite flows (Tmyt, Tmr2–Tmr9); Group 4: rhyolite flows, pyroclastic flows, and andesite flows and breccias (Tpet and Tma); Group 5: terrestrial and marine sedimentary rocks (Tps). Numerous volcanic vents have been identified within the study area, including vents for middle Miocene basalts (Tmb1 and Tmb2), possible vents for two regional ash flow tuff sheets, the 11 Ma Tmr1 and the ≥ 6 Ma Tuffs of El Canelo, as well as many vents for basaltic andesite (Tma and Tpa) and rhyolite flows (Tmr2 and Tmr9) which were erupted between 11 Ma and late Pliocene time. These vent areas were subsequently dismembered by both normal and strike–slip faulting. Depositional relationships suggest that vents for some of the regional ash flow tuffs were located south or east (Tmr4) and south (Tpet) of the study area.

Some of the 6 Ma tuffs of Group 3 (Tmr3a, Tmr3b, and Tmr4) thicken dramatically southward across an inferred normal fault system in the Dead Battery Canyon/El Coloradito area which may have originated as a caldera boundary prior to 6 Ma. The younger Group 3 units (Tmr6, Tmr7, Tmr8, and Tmr9) are largely confined to the southern part of the Sierra San Fermín. The spatial distribution of this part of Group 3 appears to have been structurally controlled. None of the Group 3 units except rhyolite flows Tmr9 crop out south of El Coloradito and Dead Battery Canyon. They have either been faulted and buried, along with batholithic rocks and older Tertiary units, or they were never deposited. The faults that offset Group 3 units were reactivated as left–lateral strike–slip faults, probably in Pliocene time. The southern part of the range is covered largely by coalesced rhyolite domes approximately 6 Ma in age, but locally as old as 8 Ma. These domes represent an effusive volcanic phase largely post–dating the major episode of normal faulting and explosive volcanism at about 6 Ma.

Stratigraphic evidence suggests limited volcanism between 11 and 6 Ma, but the evidence for a regional hiatus in deposition is equivocal. The scarcity of units between 11 and 6 Ma in age in the study area may have resulted from locally high topography in the Sierra San Fermín bordered by a basin, controlled by caldera collapse or normal faulting, in the vicinity of Arroyo Matomí.

Rocks of Group 4 are buttressed against faulted, late Miocene ignimbrites and rhyolite flows of Group 3. Group 4 rocks represent part of the mid–Pliocene volcanic sequence, which is best exposed in the Puertecitos area. Group 4 is less deformed than the late Miocene ignimbrites and flows but was nevertheless affected by normal and strike–slip faulting, which continues today.

Terrestrial sedimentary rocks of Group 5 are distinctly unconformable on late Miocene tuffs in two small basins within the Sierra San Fermín. These Pliocene (?) alluvial and lacustrine (?) deposits fill topography on faulted and eroded 6 Ma welded tuffs Tmr3b and Tmr4. Syn– and post–depositional transtensional plate boundary processes caused faulting and tilting of the alluvial section. These processes continue today.

ACKNOWLEDGMENTS

I owe a tremendous debt of gratitude to the Division of Earth and Planetary Sciences and the Seismological Laboratory at California Institute of Technology for welcoming me into their community and graciously making available many of the resources necessary for completion of this project. Kip Hodges provided access to the Cambridge Laboratory for Argon Isotope Research at the Massachusetts Institute of Technology, and he and Bill Olszewski provided patient training and assistance there. Josephine Burns, Cheryl Contopulos, Tim Johnson, D. Anne Lewis, Dan Reilly, and Susan Turbek assisted in the field. National Science Foundation grants (EAR–89–04022 and EAR–92–18381 to Joann M. Stock) and Presidential Young Investigator Award (EAR-90-58217/EAR-92-96102) to Joann M. Stock provided partial support of this research. Additional support was provided by a Geological Society of America Research Grant and Harvard University Department of Earth and Planetary Sciences Grants–in–Aid for Fieldwork.

APPENDIX A: Geochronological Techniques

$^{40}Ar/^{39}Ar$ incremental heating and total fusion ages were obtained on potassium feldspar, plagioclase, biotite, or whole rocks from twelve samples collected within the mapped area. Samples of ignimbrites were collected from unwelded bases and tops or vitrophyric zones where possible. Whole rock specimens were collected from unweathered, interior portions of lava flows. Sample preparation was carried out at the California Institute of Technology, using conventional rock–crushing, sieving, heavy–liquid and magnetic techniques. Feldspar concentrates showing glass rinds and surface impurities under the petrographic microscope were etched for 10 minutes in 5% HF. Whole rock samples were washed in 5% HCl for 30 minutes to remove calcite.

Argon extractions and analyses were done at the Cambridge Laboratory for Argon Isotope Research (CLAIR) at Massachusetts Institute of Technology using techniques detailed in Hodges (1994). The CLAIR facility comprises a MAP 215–50 mass spectrometer, a stainless steel extraction line (with SAES AP–10 Al–Zr and SAES 172 Fe–V–Zr getters), laser sample chamber, and double–vacuum resistance furnace. Evolved gas is analyzed with an electron multiplier for laser samples and a Faraday detector for furnace samples.

All samples were encapsulated in Al (commercial grade) foil, wrapped in Cd foil to reduce neutron–induced ^{40}Ar production, packed into aluminum disks, and cold–welded in an aluminum vial. The samples were irradiated for 7 hours, for an integrated power of 14 MW, in the core of the McMaster University nuclear reactor in Hamilton, Ontario, Canada. The neutron–flux parameter, J, was calculated from multiple laser analyses of two interlaboratory standards [MMhb–1 hornblende, 520.4 Ma (Samson and Alexander, 1987) and Fish Canyon tuff sanidine, 20.8 Ma (Cebula *et al.*, 1986)]. The mean J value was 0.00165 ± 0.000046, essentially constant over the length of the disks containing the Sierra San Fermín samples. Neutron–induced interfering reactions were monitored with K_2SO_4, CaF_2, and BaCl, irradiated in the package with the unknown samples. Correction factors for $(^{40}Ar/^{39}Ar)_K$, $(^{36}Ar/^{37}Ar)_{Ca}$, and $(^{39}Ar/^{37}Ar)_{Ca}$ were established by analysis of the salts at CLAIR.

Feldspar laser samples were partially degassed with a defocused laser beam at 0.4 W for 2 minutes to remove the atmospheric ^{40}Ar component (after Pringle *et al.*, 1991). This gas was not measured. The partly degassed feldspars were then fused with a laser beam at 20W. During the laser experiments, typical blanks for M/e 40, 39, 38, 37, and 36 (moles) were less than 9×10^{-16}, 2×10^{-16}, 3×10^{-17}, 3×10^{-17}, and 2×10^{-17}.

For the samples analyzed using the resistance furnace, 50–200 mg of sample, plus encapsulating foil, were dropped into a tantalum crucible and degassed at 800 K for 5 minutes. The gas released during the cleaning step was pumped away continuously during heating and not analyzed. Following degassing, samples were heated incrementally through 3–7 temperature steps up to a maximum of 1700 K. Total blanks for the resistance furnace system were about 5 to 10 times that of the laser system.

$^{40}Ar/^{39}Ar$ data were analyzed using conventional methods. Model ages for each gas extraction were calculated assuming an initial $^{40}Ar/^{39}Ar$ value of 295.5 and assigned 2σ uncertainties reflecting propagated errors in all correction factors and the J parameter. Ages were determined from release spectra and inverse ($^{36}Ar/^{40}Ar$ vs. $^{39}Ar/^{40}Ar$) isotope correlation diagrams. Two alternative methods were used to calculate "isochrons": 1) the regression treatment of York (1966), in which errors are based on data scatter, or 2) a regression with correlated errors, in which ages and errors are based on magnitude of analytical uncertainty (York, 1969). The choice of regression method depended on the mean squared weighted deviation (MSWD) of data from the best–fit line as follows: method 2 for all samples with MSWD more than 2σ from the expected value of 1 (calculated following Wendt and Carl, 1991), and method 1 for samples with MSWD $< 1 \pm 2\sigma$.

APPENDIX B: Thin Section Descriptions

The following are thin section descriptions of samples used for geochronology.

SF–92–164 **Tmb1 basalt.** Phenocrysts, 20% total: olivine, 10%; opaques, 10%; biotite, trace. Matrix: plagioclase, 60%; clinopyroxene (augite?), 20%. Olivine up to 1.5 mm long, iddingsitized on rims and in fractures. Clinopyroxene in green, stubby prisms. Plagioclase in laths. Biotite in hexagonal plates, red in plane light. Completely crystallized, no glass. Partially trachytic.

SF–92–211a **Tmr1 vitrophyre.** Phenocrysts, 7% total: anorthoclase, 5%; clinopyroxene, <1%; magnetite, <1%; trace quantities of zircon, plagioclase, and quartz. Anorthoclase sieve–textured and resorbed. Matrix: perlitically fractured, densely welded orange glass shards with grey, grainy, submicroscopic material between shards; 3% spherulites; 10% lithic fragments, including anorthoclase–rich volcanic fragments, quartzite, and devitrified glass. Lithic volcanic fragments contain 20% anorthoclase, 1% clinopyroxene, 1% magnetite, trace olivine, and trace zircon. Anorthoclase microperthitic and sieve–textured. Olivine iddingsitized. Groundmass is extensively devitrified. No primary structures (e.g. glass shards) preserved.

SF–92–116 **Tmr1 vitrophyre.** Phenocrysts, 6% total: anorthoclase, 3%; plagioclase, 1%; augite, <1%; magnetite, <1%; trace quantities of diopside and hypersthene. Resorption, Carlsbad twinning, and sieve texture in anorthoclase (largest phenocrysts up to 2 mm). Matrix: densely welded reddish–brown glass shards with white edges, pumice lapilli extremely flattened (25:1 aspect ratio). Lithic volcanic fragments comprise 2%.

SF–92–68 **Tma.** Phenocrysts, 10% total: basaltic hornblende, 6%; augite, 2%; magnetite, 2%; plagioclase, 1%;

quartz, <1%; traces of diopside and hypersthene. Magnetite dispersed and replacing basaltic hornblende. Matrix: predominantly plagioclase laths and some pyroxene. Trachytic.

SF–92–64 **Tmr3b, pumice lumps from unwelded top.** Phenocrysts, 15% total: anorthoclase + plagioclase + quartz = 14%; augite, 1%; traces of muscovite, calcite (filling interstices in vesiculated glass) and zircon. Anorthoclase > plagioclase > quartz. Augite oxidized at rims. Matrix: unwelded, vesiculated, clear glass, speckled with opaques.

SF–92–121 **Tmr3b, basal vitrophyre.** Phenocrysts, 9% total: anorthoclase + plagioclase + quartz = 7%; opaques, 1%; augite, <1%. Anorthoclase > plagioclase > quartz. Matrix: densely welded brown glass, perlitically fractured. Pumice lapilli comprise 2–3% and lithic fragments 8%. Lithics include andesite, flows, and tuffs.

SF–92–102 **Tmr8, pumice lumps.** Phenocrysts, 3% total: plagioclase, 2%; trace quantities of alkali feldspar and hypersthene. Alkali feldspar microperthitic. Matrix: colorless, vesiculated glass with dispersed opaques, which give the glass a streaky clear/brown appearance.

SF–92–108 **Tpet lower, basal orange glass.** Phenocrysts, 7% total: plagioclase, 5%; clinopyroxene (augite ± diopside), 1%; opaques, <1%; traces of hornblende, fayalite, and biotite. Fayalites have oxidized rims. Matrix: incipiently welded, bright orange, angular glass shards. No eutaxitic foliation. Shard orientation random. Lithic fragments (3%) include devitrified glass and andesite.

SF–92–110 **Tpet upper, basal black vitrophyre.** Phenocrysts, 8% total: plagioclase + quartz = 5–6%; augite, 1-2%; opaques, 1%. Matrix: incipiently welded, reddish–brown glass shards. Colorless–glass pumice lapilli comprise 2%.

SF–92–96 **Tpa.** Phenocrysts, 27% total: plagioclase, 20%; hypersthene, 3%; magnetite, 2-3%; augite, 1%; trace alkali feldspar (?). Groundmass: plagioclase, 60%; pyroxene, 13%; interstitial glass. No apparent flow foliation. Very clean sample.

APPENDIX C: Measured Sections

Composite stratigraphic sections in the central Sierra San Fermín west of El Coloradito beach camp, northern Baja California. Measured by C. J. Lewis, T. Johnson, and D. A. Lewis, using tape, compass, and eye–level sighting, on December 12–13, 1992. Sections located in Bahía Santa María [H11B67] 1:50,000 topographic quadrangle, published by DETENAL, Mexico.

Measured section 1 of Tmr1–Tmyt–Tmr3a–Tmr3at–Tmr3b, El Coloradito area

BOTTOM OF SECTION: UTM coordinates $^{33}82^{300}$ m N, $^{7}17^{300}$ m E, at elevation 280 m.

Underlain by Tmvs

Tmr1 (welded rhyolite tuff)

18.8 m No vitrophyre exposed at base. Red lithophysal grades upward into purplish grey, eutaxitically foliated, densely welded tuff, and vapor–phase crystallized tuff. Fiamme contain vapor phase minerals. Top of tuff eroded off before deposition of overlying unit.

Total thickness of Tmr1: 18.8 m

Tmyt (bedded yellow tuffs)

17.1 m Yellow–weathering, planar–bedded, cross–bedded, and massive, reworked tephra and thin tuffs. 3–cm thick lapilli bed at base of section. At least one tuff has brown surge deposits at base (low–angle truncations). Most units contain dark reddish brown lithic fragments (dacitic tuffs?). Section includes a 2–m thick, brown, lithic– and crystal–rich, finely laminated, medium–grained tuffaceous sandstone. This unit grades upward into a 1–m thick, creamy beige colored, coarse sandstone containing 50% lithic clasts, overlain by 1–m thick, yellow–weathering lithic tuff. Section also includes thinly bedded, reworked ash, lapilli, and lithic sandstone with thin conglomerate beds and brecciated conglomerate (angular gravel) in yellow–weathering matrix. Top 2 m includes a lithic–rich, coarse sand–sized tuff and some reworked tephra.

Total thickness of Tmyt: 17.1 m

Tmr3a (welded rhyolite tuff)

7.3 m Base of tuff is yellow–weathering and 50% lithic fragments. Grades upwards into slightly welded, orange weathering, lithic–lapilli tuff (~10 % lithic fragments), with 3–4 cm thick lithic concentration zones. Grades upward into reddish brown, moderately welded, devitrified tuff (~10% lithic fragments), brown-weathering devitrified tuff, dark red–weathering devitrified tuff, light brown vapor phase crystallized tuff, and unwelded tuff with pumice lapilli weathering out and lithic fragments left as knobs. These are zonal variations in a relatively thin tuff.

Total thickness of Tmr3a: 7.3 m

Tmr3at (bedded tephra)

2.0 m Multiple thin brown and yellow–weathering tuffs, some with lithic fragments concentrated at base, some with finely laminated tephra at base.

Total thickness of Tmr3at: 2.0 m

Tmr3b (welded rhyolite tuff)

13.3 m Yellow–weathering, unwelded, lithic–lapilli tuff (lithic fragments gravel-sized) grading upward into orange–weathering unwelded tuff, brown, glassy, moderately welded tuff (lithic content increases in this zone to ~10%; lithic fragments increase in size to about 3–4 cm across),

dark red devitrified tuff, and (no clear boundary) dark red devitrified tuff with vapor phase crystallized lapilli. Top removed by fault.

Total thickness of Tmr3b: 13.3 m

TOP OF SECTION

Measured section 2 of Tmr1–Tmyt–Tmr3a–Tmr3at-Tmr3b–Tmr4, El Coloradito area

BOTTOM OF SECTION: UTM coordinates $^{33}82^{300}$ m N, $^{7}14^{400}$ m E, at elevation 460 m.

Underlain by Tmvs

Tmr1 (welded rhyolite tuff)

0.1 m Orange slightly welded ash.

0.4 m Black vitrophyre (dark brown up into black).

0.4 m Smooth red devitrified tuff with big (several cm diameter) lithophysae.

0.8 m Red lithophysal with cm–scale lithophysae lined with felsic crystals.

3.9 m Red–brown weathering somewhat lithophysal tuff grading upwards into heavily devitrified and vapor phase crystallized zone.

Total thickness of Tmr1: 5.6 m

Fault cuts out tephra between Tmr1 and Tmr3a as well as base of Tmr3a. Depositional contact known to be unconformable from adjacent outcrops.

Tmr3a (welded rhyolite tuff)

6.3 m Orange–brown weathering, lapilli tuff with a few % lithic fragments, including tonalite, andesite, plagioclase–rich tuff, and devitrified rhyolite glass (base of tuff cut out by fault). Welding increases upsection (flattened lapilli).

1.6 m Dark red, crystal–rich, densely welded, devitrified zone in which lapilli weather orange.

7.3 m Upper part of same tuff. Much more lithic–rich (8–10%, including many kinds of volcanic clasts), orange–brown weathering, partially welded, with reddish purple matrix and vapor phase crystallization within lapilli.

Total thickness of Tmr3a: 15.2 m

Tmr3at (bedded tephra)

0.5 m Pink-weathering, unwelded ashflow tuff with 5% pink lapilli and about 3% lithic fragments (gravel-sized and smaller).

0.3 m Airfall lapilli and ash beds, yellow–weathering.

0.7 m Orange–brown weathering lapilli tuff, slightly foliated, with oriented pumice and discontinuous grain size variations; lapilli weather out to make holes.

Total thickness of Tmr3at: 1.5 m

Tmr3b (welded rhyolite tuff)

3.7 m Yellow–weathering (cream colored on fresh surfaces), unwelded, crystal rich, ash flow tuff.

5.6 m Eutaxitically foliated beige–orange glass, with 2–3% lithic fragments. Grades up into (about half of this horizon) partially welded (slight eutaxitic foliation), pinkish–beige, vapor phase crystallization zone.

2.2 m Dark red, devitrified tuff, with lithic fragments up to 5 cm x 3 cm, and lithophysae lined with vapor phase crystals; this zone contains at least 10% lithic fragments and no apparent eutaxitic foliation.

7.1 m Red devitrified tuff without lithophysae, containing all manner of dacitic (?) to rhyolitic, andesitic, and basaltic lithic fragments.

24.2 m Vapor phase crystallized, poorly to partially welded, light reddish purple tuff with orange–brown weathering, partially flattened lapilli. Some lithic concentration zones. [Note: Probably some duplication here due to faulting; not more than 5 m added.]

Fault.

9.3 m Beige, orange, and black weathering, partially welded (lapilli slightly flattened) tuff. Uppermost part is beige, unwelded and punky, probably vapor phase crytallized. Symmetric zonation very clear in this tuff.

Total thickness of Tmr3b: 52.1 m

Tmr4 (welded rhyolite tuff)

0.05 m Orange ash.

0.1 m Red glass with black fiamme.

4.3 m Black vitrophyre, possibly rheomorphic (strong lineated texture). This zone is crystal poor and contains <1% lithic fragments. Top 1 m of vitrophyre has orange spherulites up to 3 cm across.

4.3 m Reddish brown, devitrified glass with ~10% lapilli (large aspect ratio indicates dense welding) and a few large lithophysae.

6.5 m Dark purple–brown (almost black) zone with big lapilli (up to 8 cm x 2 cm) and baseball–sized lithophysae with concentric rings of vapor phase crystals. This zone is strongly foliated and contains ~40% lapilli.

2.2 m Purple, densely welded zone with strongly flattened lapilli and smoother texture than zone below. Lapilli are orange on fresh surfaces but weather dark brownish orange.

10.8 m Similar to zone below but platier weathering, and lapilli replaced by vapor phase crystals.

16.6 m Purple to reddish–brown, devitrified, vapor phase crystallized zone with streaky eutaxitic foliation. Very strongly foliated with highly flattened lapilli. Grades upwards into very light purple tuff with brown fiamme, streaky eutaxitic foliation, and a few lithophysae that foliation wraps around. Unwelded top removed by erosion.

Total thickness of Tmr4: 44.9 m

TOP OF SECTION

Measured section of Tmr4–Tmr5–Tmr6–Tmr7–Tmr9, Dead Battery Canyon area

BOTTOM OF SECTION: UTM coordinates $^{33}82^{300}$ m N, $^{7}14^{400}$ m E, at elevation 380 m.

Underlying unit not observed. Base of Tmr4 not exposed.

Tmr4 (welded rhyolite tuff)

~8 m Orange–weathering (light purple on fresh surface), non–foliated, crystal–poor, devitrified and vapor phase crystallized tuff. 3% lithic fragments (various volcanic aphanites), <2 cm long typically but a few up to 3 cm. 4% orange pumice lapilli, ≤6 cm long. Weathers lumpy with holes where pumice weathers out.

Tmr5 (welded rhyolite tuff)

1 m No vitrophyre at base. Base is dark red, devitrified and eutaxitically foliated with a rough (matte) surface texture.

20 m Dark red, strongly foliated, platy weathering tuff. Foliation results from vapor phase concentrations. Central part of section, foliation spaced more widely, resulting in slabby weathering. This part of tuff appears mottled; it has zones of dark red and purple, perhaps due to some oxidation process. Lithic fragments present in trace quantity.

10 m Smooth, porcelainous tuff with discontinuous vapor phase concentration zones spaced ~20 cm apart. Several per cent pumice lapilli (not visible lower in section because of vapor phase foliation). Grades upward into grey, devitrified and vapor phase crystallized tuff with ashy appearance.

5 m Unwelded, extensively devitrified, and cavernous weathering.

TOTAL THICKNESS of Tmr5: 36 m

Tmr6 (welded rhyolite tuff)

1.6 m No basal vitrophyre. Dark purplish red, densely welded, devitrified base with 5% phenocrysts and 2% each lithic fragments and pumice lapilli.

7.9 m Orange-weathering, densely welded, eutaxitically foliated, and slabby-weathering tuff.

9.5 m Vapor phase concentration zones laced through dark purplish–red, densely welded tuff (many anastamosing, thin white zones). Weathers into irregular slabs with rounded edges. Color grades upwards into grayish–purple.

9.5 m Slabby weathering, densely welded but only slightly foliated tuff. More pumice lapilli than lower in tuff (10%).

6.3 m Moderately welded tuff very rich in lithic inclusions (30%), ≤30 cm x 4 cm. Inclusions extensively devitrified with vesicles filled by vapor phase minerals. Lithics are monolithologic and probably cognate.

3.2 Unwelded, brown weathering tuff very rich in pumice lapilli.

TOTAL THICKNESS of Tmr6: 38.0 m

Tmr7 (unwelded rhyolite tuffs)

8.30 m Thinly bedded tephra (maximum bed thickness 10 cm). Beige, sandy matrix with yellow–weathering pumice lapilli, grey, feldspar–rich pumice lapilli (≤4 cm long), lithic fragments, and crystals (feldspar and biotite). Some beds contain 30% lithic fragments plus pumice lapilli. Lithic fragments include foliated rhyolite, aphanites, and welded tuffs. A few large pumice bombs (≤20 cm) in otherwise size–sorted, planar bedded deposits suggests some beds may be airfall deposits. [Note: In other localities, this unit is comprised of planar bedded tephra with lenses of tuffaceous sandstone. Rounded glass fragments, pumice lapilli, and blocks of unwelded, vapor phase devitrified tuff may have been reworked from the unwelded top of the underlying Tmr6.]

2.75 m Brown–weathering, unwelded pumice flow. 25% brown–weathering (grey on fresh surface), feldspar-rich pumice, ≤10 cm across. 50% small (<1 cm long) pumice and lithic lapilli and crystals. 25% ash matrix. Lithic fragments include 1% black vesiculated glass. White base grades upwards into beige and thence into bright pink ignimbrite. Top is oxidized, probably by heat from emplacement of overlying ignimbrite. No bedding or foliation.

3.64 m Brown–weathering, unwelded pumice flow. Very similar to underlying brown pumice flow but with pumice concentration zones, which form slope breaks. Pumice blocks ≤30 cm across. Contains more lithics (~10% total) than the underlying pumice flow, including various volcanic lithologies. Brown silicified base ~2 cm thick. Flow thickens to the east.

9.13 m Brown–weathering, unwelded pumice flow. Pinkish base grades upwards into brown tuff and thence into white top. Basically the same as underlying pumice flows except that this one has lithic concentration zones, containing primarily flow–banded rhyolites and dark purplish–

black aphanites. Lithic inclusions ≤6 cm long. Most of tuff impoverished of lithics, although there are two principal zones of lithic concentration, at the base and ~1 m from the top.

3.82 m Brown–weathering, unwelded pumice flow. Basically the same as the underlying pumice flows. 10% lithics throughout (various volcanic lithologies). Some faint bedding defined by grain size variations; these are correlated with color changes. 2–cm thick silicified, white and brown banded, basal ash, which forms a slope break. White band 15 cm thick grades up into pink band 25 cm thick, which grades up into a brown band with discontinuous white bands. This tuff contains some pumice concentration zones, especially the top 1 m. A 10–cm wide, white, clay alteration zone enriched in pumice occurs 50 cm down from the top.

0.04 m Brown ash.

9.96 m Brown–weathering, unwelded pumice flow. Basically the same as the underlying pumice flows. Thin, silicified, pink and white banded base grades up into 10–cm thick white zone. Rest is brown–weathering except for the top 1 m, which is mustard yellow. Pumice in this flow generally smaller than in underlying pumice flows except for some pumice concentration zones in which pumice lapilli are as large as 12 cm. This tuff is cut by a fault; may be thinner than measured. May include more than one eruptive unit; difficult to tell due to poor exposure beneath colluvium.

TOTAL THICKNESS of Tmr7: 37.64 m

Tmr9 (rhyolite flows)

~15 m Ashy, lithic–rich base of rhyolite flow section. Looks like an ash flow tuff from a distance, but it is really an agglomerate of rhyolite breccia and ash. Irregularly shaped pieces of devitrified rhyolite, some having oxidized red rims. Base of this unit is pinkish–red mottled with regions of grayish–purple and brown. Structureless overall except for locally vague layering due to alignment of elongate lithic fragments. Weathers lumpy. Most rhyolite fragments are spherulitically altered. Matrix is brown ash. This unit is poorly exposed and cut by faults. Note: This unit might be the same as Tmr8.

1 m Base of flow is rhyolite breccia in grey lithified ash matrix. Contains about 25% spherulitically altered rhyolite, some of it flow banded.

~1 m Lithified breccia-randomly oriented blocks welded together.

~40 m Dark reddish–purple stony rhyolite. Highly contorted flow foliation.

TOTAL THICKNESS of Tmr9: 57 m

BIBLIOGRAPHY

ANDERSEN, R. L., 1973. Geology of the Playa San Felipe quadrangle, Baja California, Mexico. M.S. Thesis, California State University San Diego, 214 pp.

ANDERSON, P. V., 1982. Pre-batholithic stratigraphy of the San Felipe area, Baja California, Mexico. M.S. Thesis, San Diego State University, 100 pp.

AXEN, G., 1995. Extensional segmentation of the Main Gulf Escarpment, Mexico and United States. *Geology, 23*, 515-518.

BEST, M. G., 1982. Igneous and metamorphic petrology. San Francisco, California, W.H. Freeman and Company, 630 pp.

BOEHM, M., 1984. An overview of the lithostratigraphy, biostratigraphy, and paleoenvironments of the late Neogene San Felipe marine sequence, Baja California, Mexico, *In:* Frizzell, V. A., (eds.), Geology of the Baja California Peninsula, Los Angeles, Soc. Econ. Paleontol. Mineral., Pacific Section, 253-266.

BRYANT, B. A., 1986. Geology of the Sierra Santa Rosa basin, Baja California, Mexico. M.S. Thesis, San Diego State University, 75 pp.

CEBULA, G. T., M. J. KUNK, H. H. MEHNERT, C. W. NAESER and J. D. OBRADOVICH, 1986. The Fish Canyon tuff, a potential standard for the $^{40}Ar/^{39}Ar$ and fission track methods (abstract). *Terra Cognita, 6*, 139-140.

DOKKA, R.K. and R.H. MERRIAM, 1982. Late Cenozoic extension of northeastern Baja California. *Geol. Soc. Am. Bull., 93*, 371-378.

DORSEY, R. and B. BURNS, 1994. Regional stratigraphy, sedimentology, and tectonic significance of Oligocene-Miocene sedimentary and volcanic rocks, northern Baja California, Mexico. *Sed. Geol., 88*, 231-251.

FISHER, R. V., 1966. Rocks composed of volcanic fragments. *Earth Sci. Rev., 1*, 287-298.

GABB, W. M., 1882. Notes on the geology of Lower California. *Calif. Geol. Surv., Geology, 2*, 137-148.

GASTIL, G., D. LEMONE and W. STEWART, 1973. Permian fusilinids from near San Felipe, Baja California. *Am. Assoc. Petrol. Geol. Bull., 57*, 746-747.

GASTIL, R. G. and D. KRUMMENACHER, 1977. Reconnaissance geology of coastal Sonora between Puerto Lobos and Bahía Kino. *Geol. Soc. Am. Bull., 88*, 189-198.

GASTIL, R. G., D. KRUMMENACHER and STUDENTS AT SAN DIEGO STATE UNIVERSITY, 1974. Reconnaissance geologic map of coastal Sonora between Puerto Lobos and Bahía Kino. Geol. Soc. Am. Map and Chart Series MC-16.

GASTIL, R. G., G. D. KRUMMENACHER and J. MINCH, 1979. The record of Cenozoic volcanism around the Gulf of California. *Geol. Soc. Am. Bull., 90*, 839-857.

GASTIL, R. G., R. P. PHILLIPS and E. C. ALLISON, 1975. Reconnaissance geology of the state of Baja California. Geol. Soc. Am. Mem. 140, 170 pp.

HAMILTON, W., 1971. Recognition on space photographs of structural elements of Baja California. U.S. Geol Surv. Prof. Pap., 26 pp.

HILDRETH, W., 1979. The Bishop Tuff: Evidence for the origin of compositional zonation in silicic magma chambers. *Geol. Soc. Am. Spec. Pap. 180*, 43-73.

HODGES, K., W. E. HAMES, W. OLSZEWSKI, B. C. BURCHFIEL, L. H. ROYDEN and Z. CHEN, 1994. Thermobarometric and $^{40}Ar/^{39}Ar$ geochronologic constraints on Eohimalayan metamorphism in the Dinggyê area, southern Tibet. *Contrib. Mineral. Petrol., 117*, 151-163.

KERR, D. R., 1984. Early Neogene continental sedimentation in the Vallecito and Fish Creek Mountains, western Salton Trough, California. *Sed. Geol., 38*, 217-246.

LEWIS, C. J., 1993. Paleomagnetic evidence of localized rotations during Neogene extension in the Sierra San Fermín, northeastern Baja California, Mexico. Geol. Soc. Am. Abstracts with Programs, 25, A-283.

LEWIS, C. J., 1994. Constraints on extension in the Gulf Extensional Province from the Sierra San Fermín, northeastern Baja California, Mexico. PhD Thesis, Harvard University, 361 pp.

MARTIN BARAJAS, A. and J. M. STOCK, 1993. Estratigrafía y petrología de la secuencia volcánica de Puertecitos, noreste de Baja California. Transición de un arco volcánico a rift. *In:* Delgado Argote, L. A., and A. Martín Barajas, (eds.), Contribuciones a la Tectónica del Occidente de México, Unión Geofísica Mexicana, Monografía No. 1, 66-89.

MARTIN-BARAJAS, A., J. M. STOCK, P. LAYER, B. HAUSBACK, P. RENNE and M. LOPEZ-MARTINEZ, 1995. Arc–rift transition volcanism in the Puertecitos volcanic province, northeastern Baja California, Mexico. *Geol. Soc. Amer. Bull., 4*, 407-424.

MARTIN-BARAJAS, A., M. TELLEZ DUARTE and G. RENDON MARQUEZ, 1993. Estratigrafía y ambientes de depósito de la secuencia marina de Puertecitos, NE de Baja California. Implicaciones sobre la evolución del margen Occidental de la depresión del golfo. *In:* Delgado Argote, L. A. and Martin-Barajas, A., (eds.), Contribuciones a la Tectónica del Occidente de México, Unión Geofísica Mexicana Monografía No. 1, 66-89.

MELBOURNE, T., J. HOLT and J. M. STOCK, 1993. Paleomagnetic investigation of the Puertecitos Volcanic Region, B. C. Peninsular Geological Society, Second International Meeting on Geology of the Baja California Peninsula, Ensenada, B.C.N., Mexico, abstracts, 62.

NAGY, E. A., 1995. Implications of $^{40}Ar/^{39}Ar$ geochronology on Miocene volcanics from the north-central Puertecitos Volcanic Province, northeastern Baja California. Peninsular Geological Society, Third International Meeting on Geology of the Baja California Peninsula, La Paz, B.C.S., Mexico, abstracts, 130-131.

NEUHAUS, J. D., 1989. Volcanic and nonmarine stratigraphy of southwest Isla Tiburón, Gulf of California, Mexico. M.S. Thesis, San Diego State University, 170 pp.

PRINGLE, M. S., H. STAUDIGEL and J. GEE, 1991. Jasper Seamount: Seven million years of volcanism: *Geology, 19*, 364-368.

RUISAARD, C. I., 1979. Stratigraphy of the Miocene Alverson Formation, Imperial County, California. M.S. Thesis, San Diego State University, 125 pp.

SAMSON, S. D. and E. C. ALEXANDER, 1987. Calibration of the interlaboratory $^{40}Ar/^{39}Ar$ standard, MMhb-1. *Geochim. Cosmochim. Acta, 66*, 27-34.

SMITH, J. T., J. G. SMITH, J. C. INGLE, R. G. GASTIL, M. C. BOEHM, J. ROLDAN Q. and R. E. CASEY, 1985. Fossil and K-Ar age constraints on upper middle Miocene conglomerates, SW Isla Tiburón, Gulf of California. Geol. Soc. Am. Abstracts with Programs, 17, 409.

SOMMER, M. A. and J. GARCIA, 1970. Potassium-argon dates for Pliocene rhyolite sequences east of Puertecitos, Baja California. Geol. Soc. Am. Abstracts with Programs, 2, 146.

STEIGER, R. H. and E. JAEGER, 1977. Subcommission on geochronology; convention on the use of decay constants in geo- and cosmochronology. *Earth and Planet. Sci. Lett., 36*, 359-362.

STOCK, J. M., 1989. Sequence and geochronology of Miocene rocks adjacent to the Main Gulf Escarpment: Southern Valle Chico, Baja California Norte, México. *Geofís. Int., 28*, 5, 851-896.

STOCK, J. M., 1993. Geology of southern Valle Chico and adjacent regions, Baja California, Mexico. Geol. Soc. Am. Map and Chart Series MCH076.

STOCK, J. M. and K. V. HODGES, 1989. Pre-Pliocene extension around the Gulf of California and the transfer of Baja California to the Pacific plate. *Tectonics, 8,* 99-115.

STOCK, J. M. and K. V. HODGES, 1990. Miocene to Recent structural development of an extensional accommodation zone, northeastern Baja California, Mexico. *Jour. Struct. Geol., 12,* 315-328.

STOCK, J. M., A. MARTIN B., F. SUAREZ V. and M. M. MILLER, 1991. Miocene to Holocene extensional tectonics and volcanic stratigraphy of NE Baja California, Mexico, *In:* Walawender, M. J. and B. B. Hanan, (eds.), Geological Excursions in Southern California and Mexico, San Diego, California, Geol. Soc. Am. Guidebook, 44-67.

WEAVER, B. F., 1981. Tertiary marine conglomerate, southwestern Tiburon Island, *In:* Ortlieb, L. and J. Roldan Q., (eds.), Geology of northwestern Mexico and southern Arizona, Mexico, D. F., Instituto de Geología, Universidad Nacional Autónoma de México, 99-103.

WENDT, I. and C. CARL, 1991. The statistical distribution of the mean squared weighted deviation. *Chem. Geol., 86,* 275-285.

Claudia J. Lewis

Department of Earth and Planetary Sciences, Harvard University, 24 Oxford St., Cambridge, MA 02138
Present Address: Departament de Geologia Dinàmica, Geofísica i Paleontologia, Universitat de Barcelona, Zona Universitaria de Pedralbes, 08071 Barcelona, Spain.